INTERNATIONAL ATOMIC ENERGY AGENCY
UNITED NATIONS EDUCATIONAL, SCIENTIFIC AND CULTURAL ORGANIZATION
INTERNATIONAL CENTRE FOR THEORETICAL PHYSICS
I.C.T.P., P.O. BOX 586, 34100 TRIESTE, ITALY, CABLE: CENTRATOM TRIESTE

UNITED NATIONS INDUSTRIAL DEVELOPMENT ORGANIZATION
INTERNATIONAL CENTRE FOR SCIENCE AND HIGH TECHNOLOGY

H4.SMR/544 - 15

Winter College on Ultrafast Phenomena

18 February - 8 March 1991

Progress in Parametric Generation and Amplification of Ultrashort Light Pulses

A. Piskarskas
Vilnius University
Laser Research Center
Vilnius, Lithuania

1

PROGRESS IN PARAMETRIC GENERATION AND AMPLIFICATION OF ULTRASHORT LIGHT PULSES

A. Piskarskas

Vilnius University
Laser Research Center
Saulėtekio ave. 9
232054 Vilnius, Lithuania

Key Points

- Short Retrospective
- Main Trends in OPA & OPO Research
- Picosecond and Femtosecond OPA & OPO
- Phase Conjugation
- Squeezing
- Four-Photon OPO
- New Pump Sources
- Applications

First Papers on OPA

- Observation of Parametric Amplification in the Optical Range / Akhmanov S.A., Kovrigin A.I., Piskarskas A.S., Fadeev V.V., Khokhlov R.V. // JETP Lett. 1965 V.2, No.7, P. 191-193.
- Measurement of Parametric Gain Accompanying Optical Difference Frequency Generation / Wang C.C., Racette G.W. // Appl. Phys. Lett. 1965 V.6, No.8, P. 196-171.

First Papers on OPO

- Tunable Coherent Parametric Oscillation in $LiNbO_3$ at Optical Frequencies / Giordmaine J.A., Miller R.C. // Phys. Rev. Lett. 1965 V.14, No.24, P. 973-976.

- Tunable Parametric Light Generator with KDP Crystal / Akhmanov S.A., Kovrigin A.I., Piskarskas A.S., Fadeev V.V., Khokhlov R.V. // JETP Lett. 1966 V.3, No.9, P. 241-245.

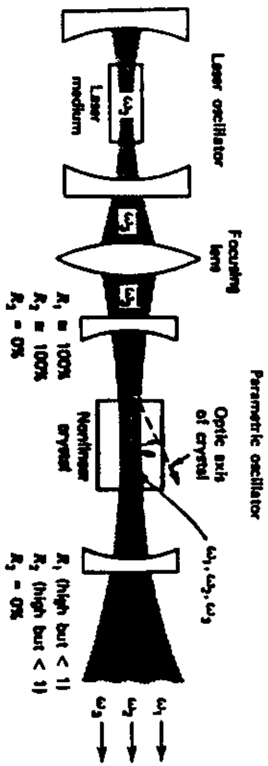

Figure Schematic diagram of an optical parametric oscillator in which the laser output at ω_3 is used as the pump. The resulting gain gives rise to oscillations at ω_1 and ω_2 (where $\omega_3 = \omega_1 + \omega_2$) in an optical cavity that contains the nonlinear crystal and resonates at ω_1 and ω_2.

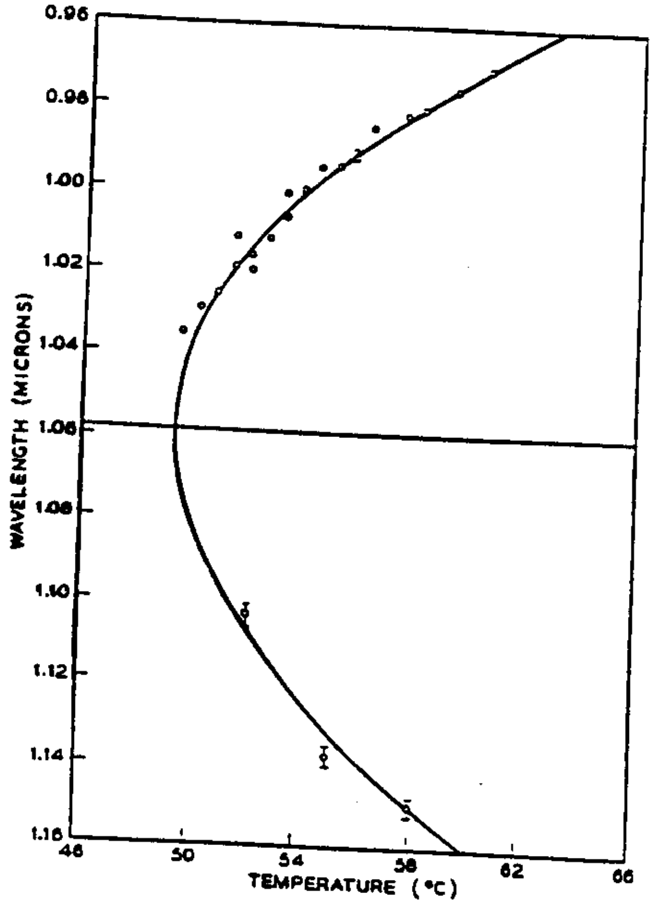

FIG. Signal and idler wavelength as a function of temperature T_2 of the oscillator crystal

(by GIORDMAINE J.E. & MILLER R.C.)

PROBLEMS TO BE SOLVED

- EXTENSION OF TUNING RANGE
  - HIGH TRANSPARENT CRYSTALS THROUGH VISIBLE, UV & IR
  - UV PUMP SOURCES
- PULSE WIDTH REDUCTION
  - Fs PUMP SOURCES
  - NEW APPROACH TO FAST PHASE CONTROL
- NARROW LINE OPO. BANDWIDTH LIMITED PULSES
  - PUMP OF HIGH TIME & SPACE COHER.
  - FILTERING
  - CAVITY STABILIZATION
- HIGH ENERGY OPO
  - TRAVELING WAVE OR NONCOLINEAR
  - CRYSTALS OF LARGE APERTURE
- THRESHOLD REDUCTION
  - NEW MATERIALS OF HIGH $\chi^{(2)}$
  - HIGH QUALITY CAVITIES (MONOLIT)
  - CONFOCAL FOCUSING
- SQUEEZING (IN PROGRESS)

EQUATIONS FOR 3-WAVE PARAMETRIC INTERACTION

$$\frac{\partial A_1}{\partial z} + \nu_1 \frac{\partial A_1}{\partial t} - \frac{i}{2} g_1 \frac{\partial^2 A_1}{\partial t^2} + \beta_1 \frac{\partial A_1}{\partial x} + \frac{i}{2k_1}\left(\frac{\partial^2 A_1}{\partial x^2} + \frac{\partial^2 A_1}{\partial y^2}\right) = -\delta_1 A_1 + \sigma_1 A_3 A_2^* \exp(-i\Delta_z z),$$

$$\frac{\partial A_2}{\partial z} + \nu_2 \frac{\partial A_2}{\partial t} - \frac{i}{2} g_2 \frac{\partial^2 A_2}{\partial t^2} + \beta_2 \frac{\partial A_2}{\partial x} + \frac{i}{2k_2}\left(\frac{\partial^2 A_2}{\partial x^2} + \frac{\partial^2 A_2}{\partial y^2}\right) = -\delta_2 A_2 + \sigma_2 A_3 A_1^* \exp(-i\Delta_z z),$$

$$\frac{\partial A_3}{\partial z} + \nu_3 \frac{\partial A_3}{\partial t} - \frac{i}{2} g_3 \frac{\partial^2 A_3}{\partial t^2} + \beta_3 \frac{\partial A_3}{\partial x} + \frac{i}{2k_3}\left(\frac{\partial^2 A_3}{\partial x^2} + \frac{\partial^2 A_3}{\partial y^2}\right) = -\delta_3 A_3 + \sigma_3 A_1 A_2 \exp(i\Delta_z z),$$

$$\frac{\partial A_1}{\partial z} + \nu_1 \frac{\partial A_1}{\partial t} - i\frac{g_1}{2}\frac{\partial^2 A_1}{\partial t^2} = -\delta_1 A_1 + \sigma_1 A_3 A_2^* \exp(-i\Delta_z z),$$

$$\frac{\partial A_2}{\partial z} + \nu_2 \frac{\partial A_2}{\partial t} - i\frac{g_2}{2}\frac{\partial^2 A_2}{\partial t^2} = -\delta_2 A_2 + \sigma_2 A_3 A_1^* \exp(-i\Delta_z z),$$

$$\frac{\partial A_3}{\partial z} + \nu_3 \frac{\partial A_3}{\partial t} - i\frac{g_3}{2}\frac{\partial^2 A_3}{\partial t^2} = -\delta_3 A_3 + \sigma_3 A_1 A_2 \exp(i\Delta_z z).$$

$$\omega_1 + \omega_2 = \omega_3$$

$$A_1 = A_{10}\,\mathrm{ch}\,m + \sqrt{\frac{\sigma_1}{\sigma_2}}\,A_{20}^*\,\mathrm{sh}\,m$$

$$A_2 = A_{20}\,\mathrm{ch}\,m + \sqrt{\frac{\sigma_2}{\sigma_1}}\,A_{10}^*\,\mathrm{sh}\,m$$

$$m = \sqrt{\sigma_1\sigma_2}\,A_{30}Z$$

$m \gg 1$, $A_2 = \sqrt{\frac{\sigma_2}{\sigma_1}}\,A_1^* \Rightarrow$ phase conjugation

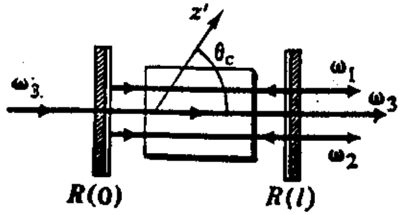
z'
θc
ω3
ω1
ω3
ω2
R(0)
R(l)

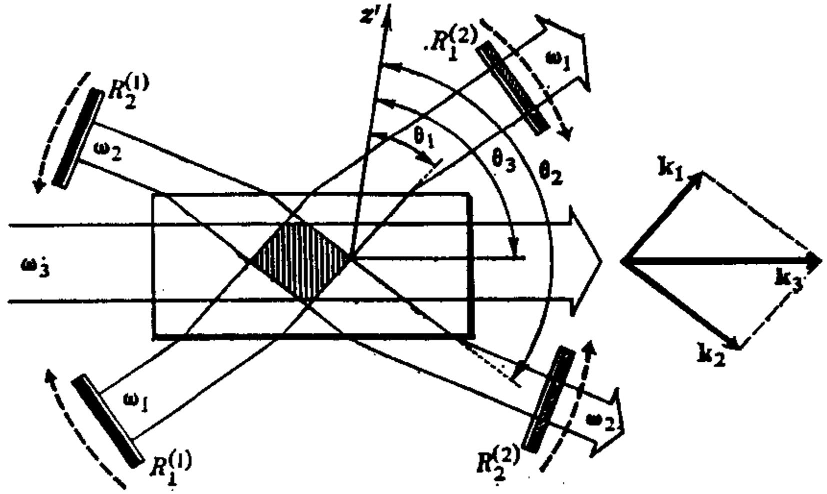
z'
R1(2)
ω1
R2(1)
ω2
θ1
θ3
θ2
ω3
k1
k3
k2
ω1
R1(1)
R2(2)
ω2

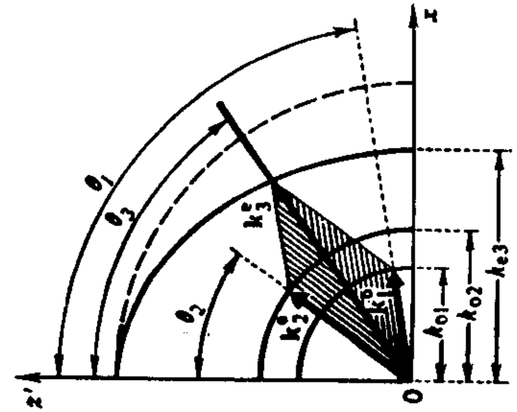
z
θ1
θ3
θ2
z'
0
ko1
ko2
ke3

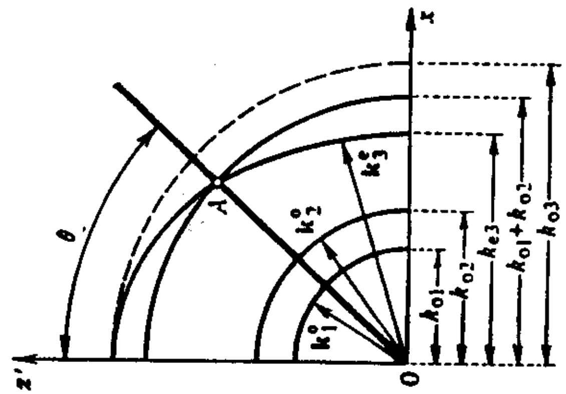
z
θ
A
z'
0
ko1
ko2
ke3
ko1+ko2
ko3

Nonlinear Crystals for SHG and OPO

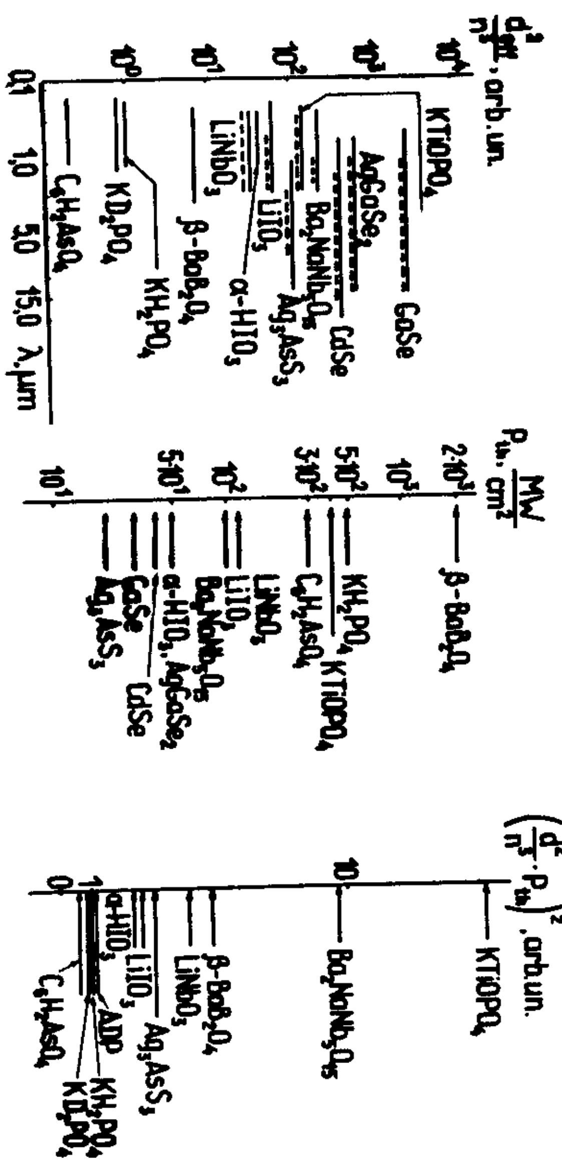

(from R.L. BYER et. al.)

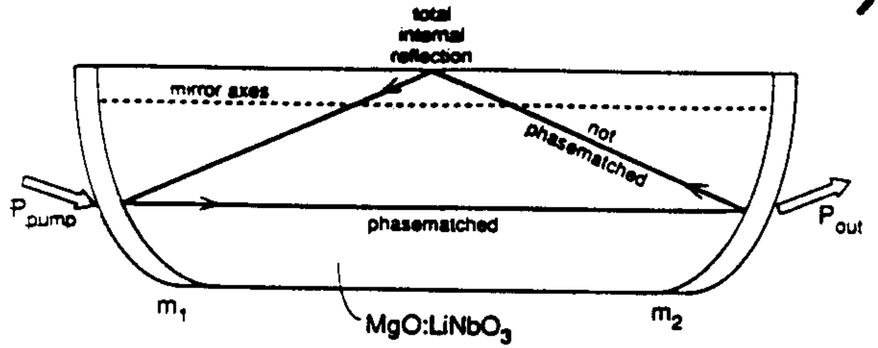

FIGURE 3.1(a). Monolithic DRO crystal cavity design. Dielectric mirrors that are highly reflective for the signal and idler and transmit the pump are deposited directly on the curved ends of the MgO:LiNbO$_3$ resonator. m1: HR 1064 nm, T = 85% 532 nm. m2: T = 0.5% 1064 nm.

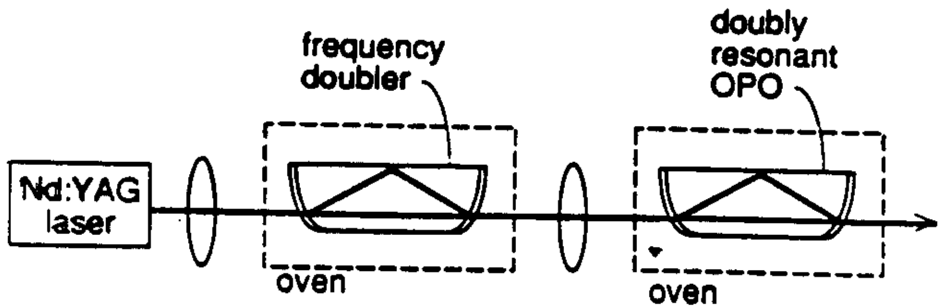

FIGURE 3.1(b). Experimental setup for the OPO showing the diode-laser-pumped Nd:YAG laser, external resonant doubler, and doubly-resonant OPO.

R = 10 mm ϕ = 27 μm (1.06 μm)

ℓ = 12,5 mm T_s = 0.5%

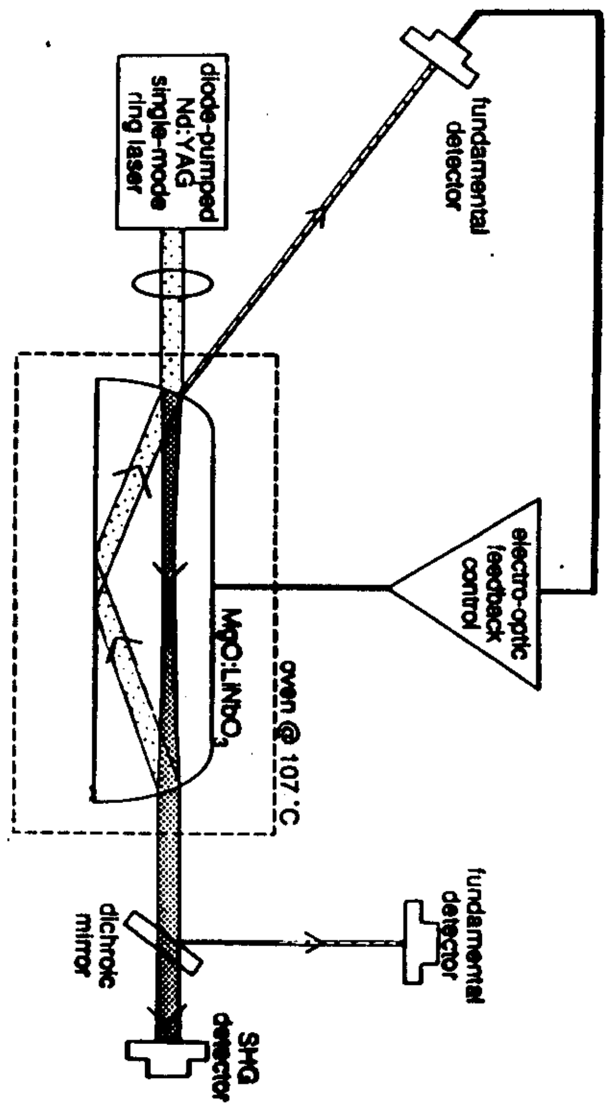

Resonant second harmonic generation from the diode-laser-pumped Nd:YAG laser. [Reproduced from Ref. 9] (BYER R.L. et.al.

$l = 12,5$ mm
$P_{1,064} = 53$ mW
$P_{0,53} = 30$ mW $\}$ $\eta = 56\%$

(by R.L. BYER et.al.)

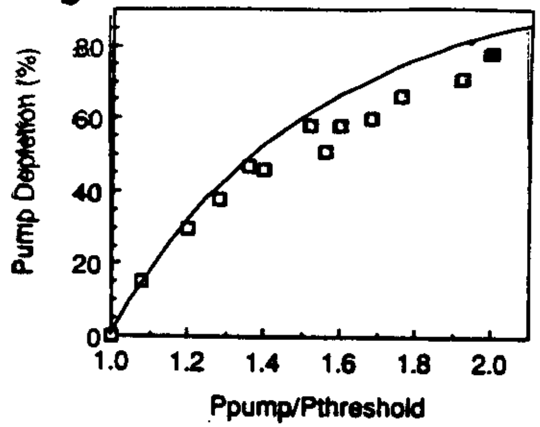

$P_t = 3,2$ m

Pump depletion of the cw DRO *vs.* number of times above threshold (pump power divided by threshold power). The solid line is the plane-wave theory after Bjorkholm (Ref. 5).

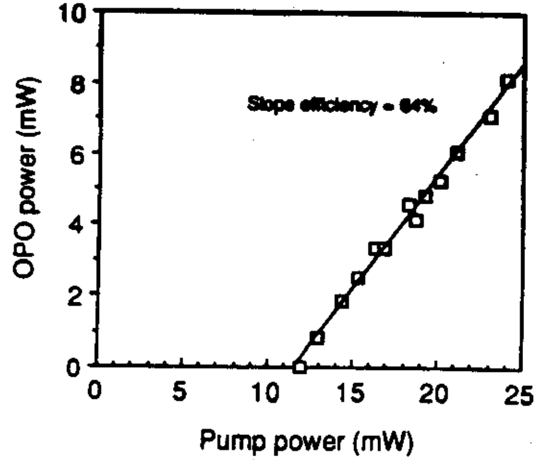

. OPO threshold and 'slope efficiency' which, surprisingly, is rather linear.

$P_{s+i} = 8.15$ mW
$P_p = 24$ mW $\}$ $\eta = 34\%$
$\eta_{\omega\to\omega_s} = 14.2\%$, $\eta_{OL} = 46\%$ from 0,

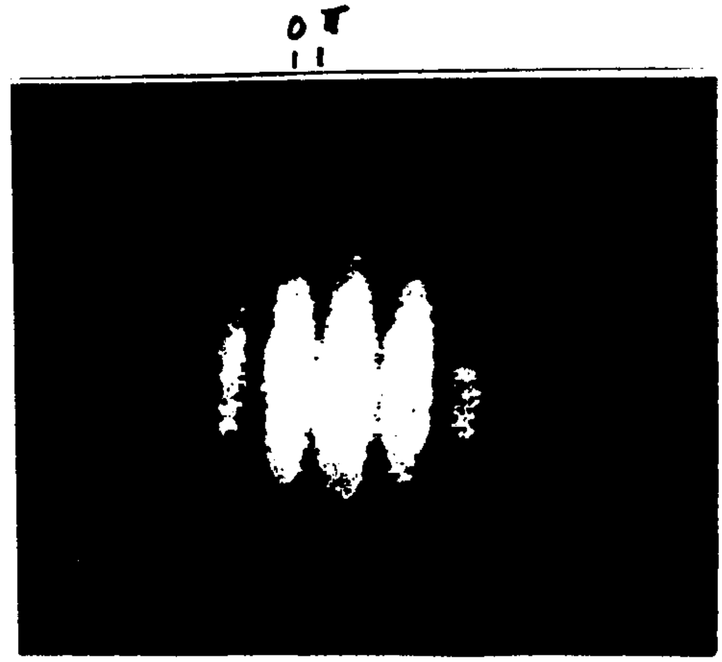

Stable fringe pattern produced by interfering the degenerate DRO beam with a reference beam from the Nd:YAG laser.

(from R. ECKARD et. al.)

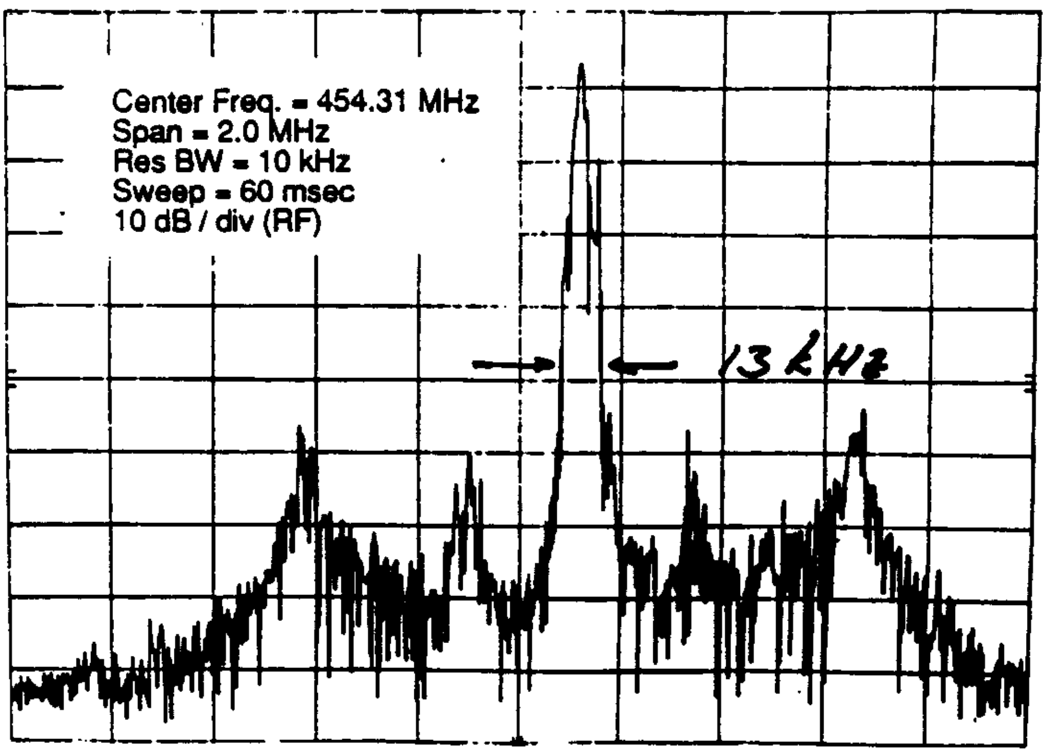

Heterodyne RF beatnote spectrum of the independent DRO signal and Nd:GGG laser oscillators. The 3 dB full width of the central peak is 13 kHz. (from R. ECKARD et. al.)

Parameters of ps CW-pumped YAG:Nd Laser

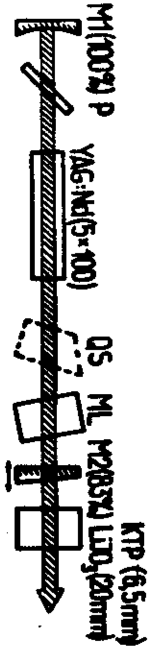

	λ = 1,064 μm				λ = 0,532 μm				λ = 0,3547 μm		
	τ, ps	P_a, W (E_t, mJ)	P_p, kW	N	τ, ps	P_a, W (E_t, mJ)	P_p, kW	N	ε, %	P_a, W (f_{QS}=1kHz)	P_p, kW
AML (f_{AM}=139 MHz)	55	8,5	1,1	∞	40	1(KTP)	0,18	∞	–	–	–
AML and QS (f_{QS}^{max}=4 kHz)	65	(1,8)	900	30	50	(0,5) (LiJO$_3$)	400	25	20 (KDP)	0,360	280

CW ps OPO Setup

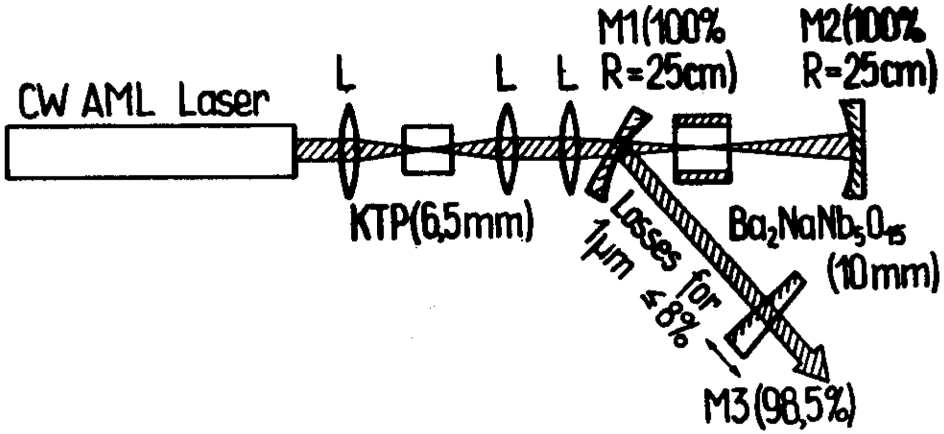

$P_{th,av}$ mW	$P_{th,p}$ W	τ, ps	Tuning range, μm	P_{av}, mW	P_p, W
28	4	≤37	0,95-1,2*	55	10

CW ps OPO: Energy Conversion; Cavity Detuning

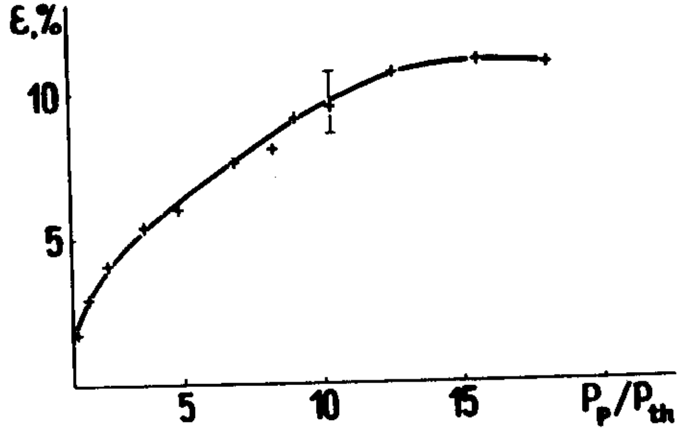

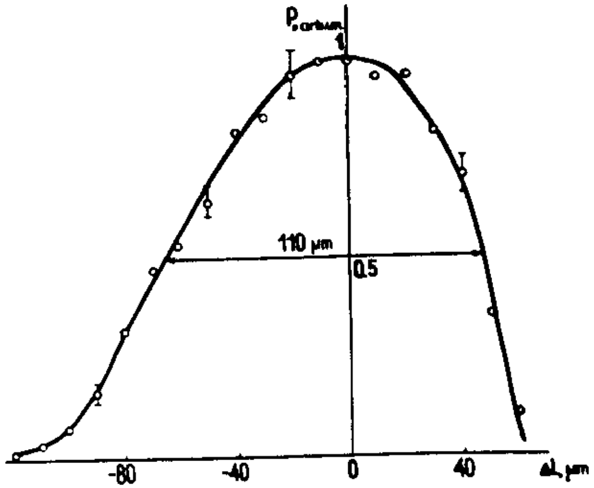

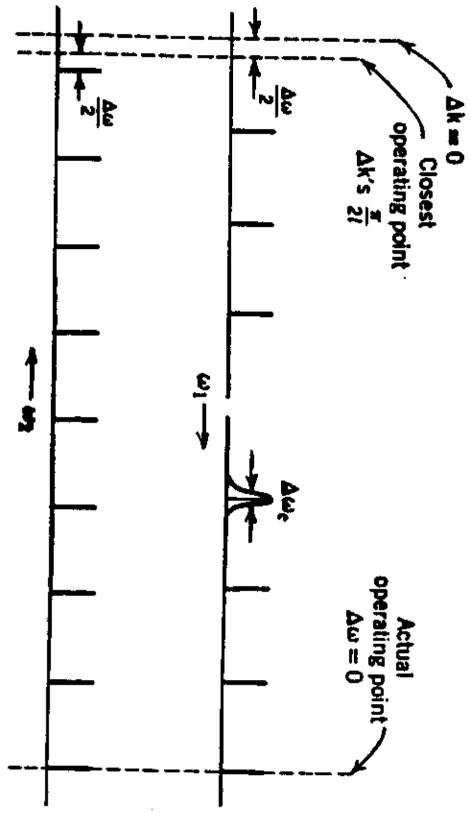

Figure - Modes in the resonator of a doubly resonant oscillator. Note that ω_1 increases to the right and ω_2 to the left. Lines vertically above each other indicate the coincidence of idler and signal modes. To the left is the point where ω_1 and ω_2 are phase matched. The closer operating point is the dotted line next to it, but the gain is higher at the point furthest to the right and this is the actual operating point. After Giordmaine and Miller, in *Physics of Quantum Electronics*, P. L. Kelley et al., Eds., McGraw-Hill, New York, 1966, p. 31.

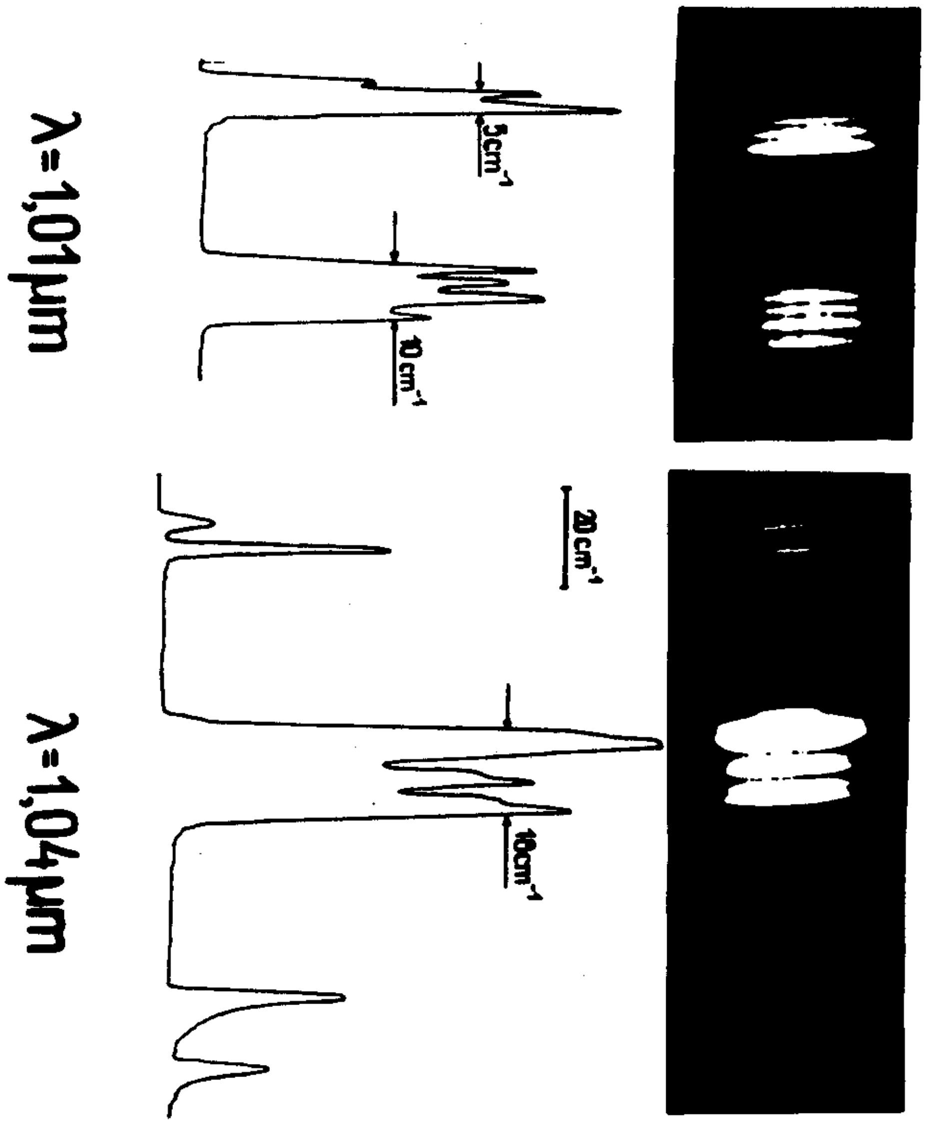

H.r.r. ps OPO Setup

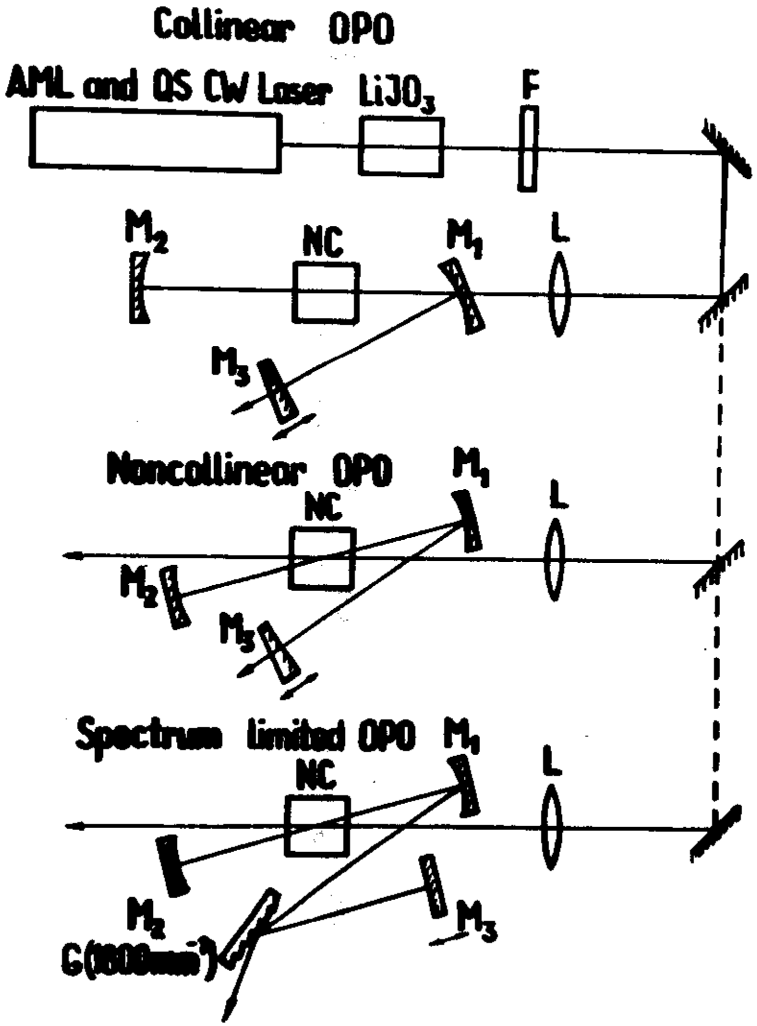

OPO Spectrum Width Dependence on the Degeneracy Parameter

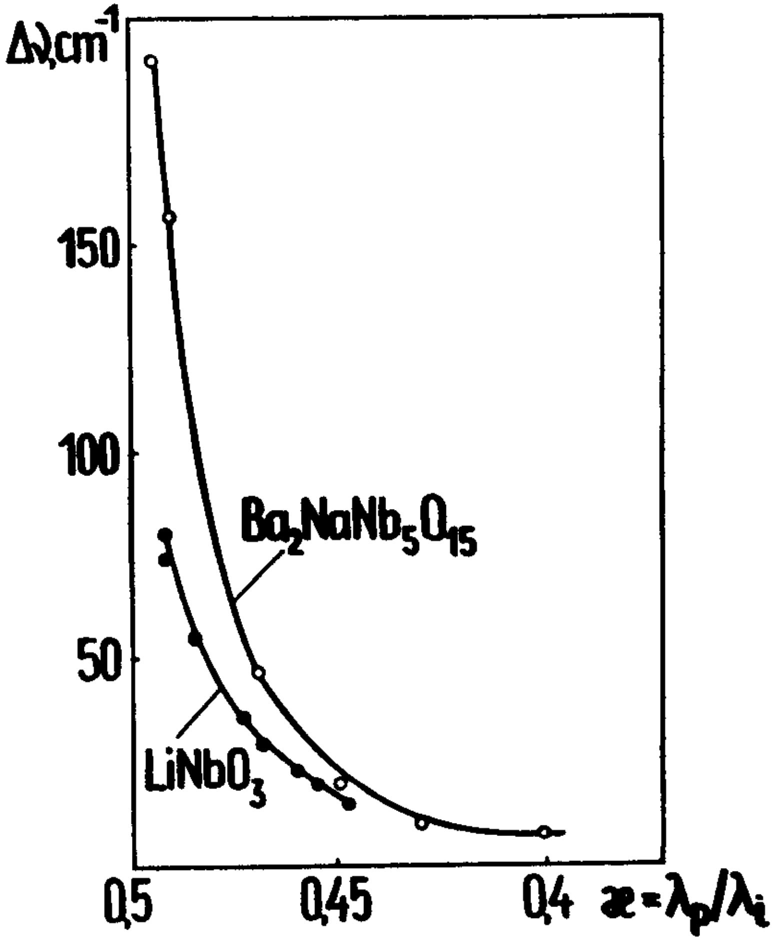

Cavity Detuning of Bandwidth Limited ps OPO

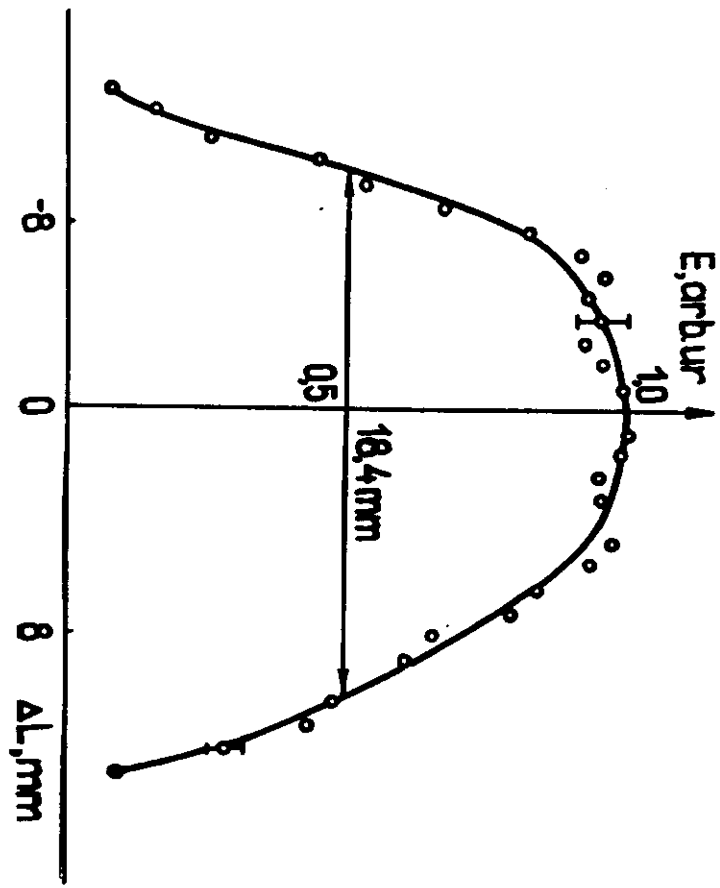

Bandwidth Limited ps OPO Spectrum

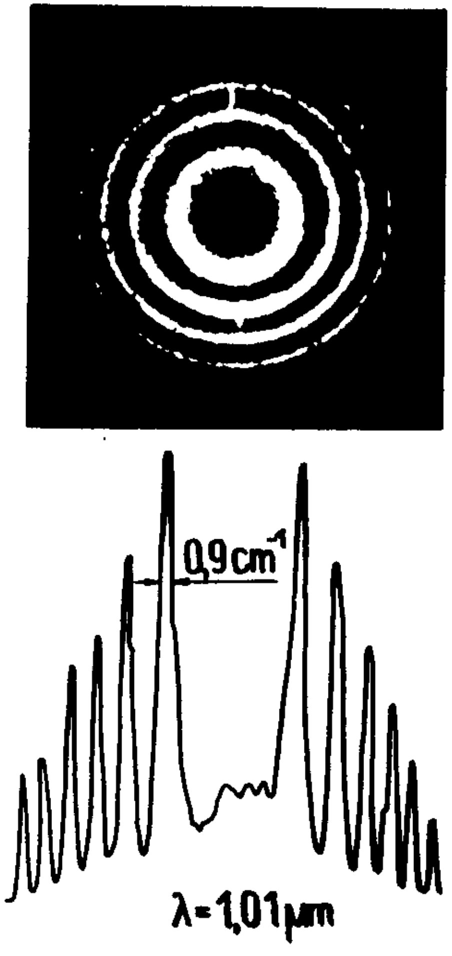

Ps OPO Pumped by TCP of AML and QS CW YAG:Nd Laser

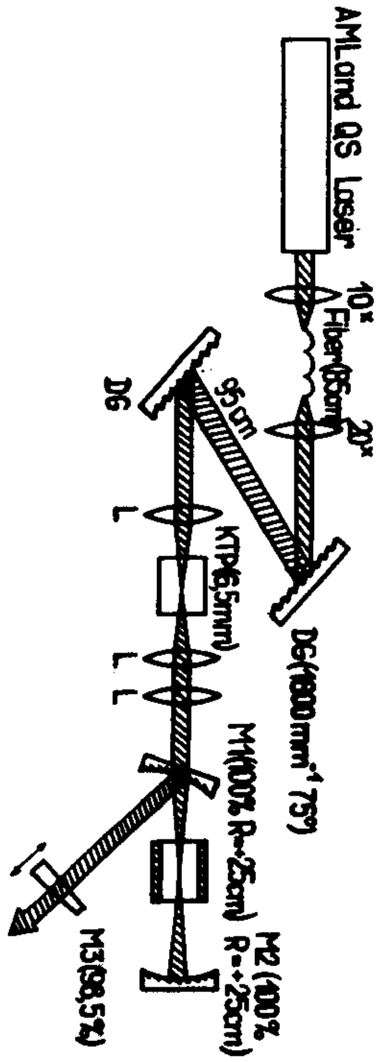

	P_{th}, kW	ε, %	τ, ps	P_p, kW	λ, μm
After compression	—	—	6	130	1,064
SH after compression	—	7	4,5	16	0,532
$Ba_2NaNb_5O_{15}$ OPO	1,1 (0,15 mW, f=1kHz)	13	3,5	3	0,95 - 1,2

Ps OPO Pumped by TCP. Spectrum

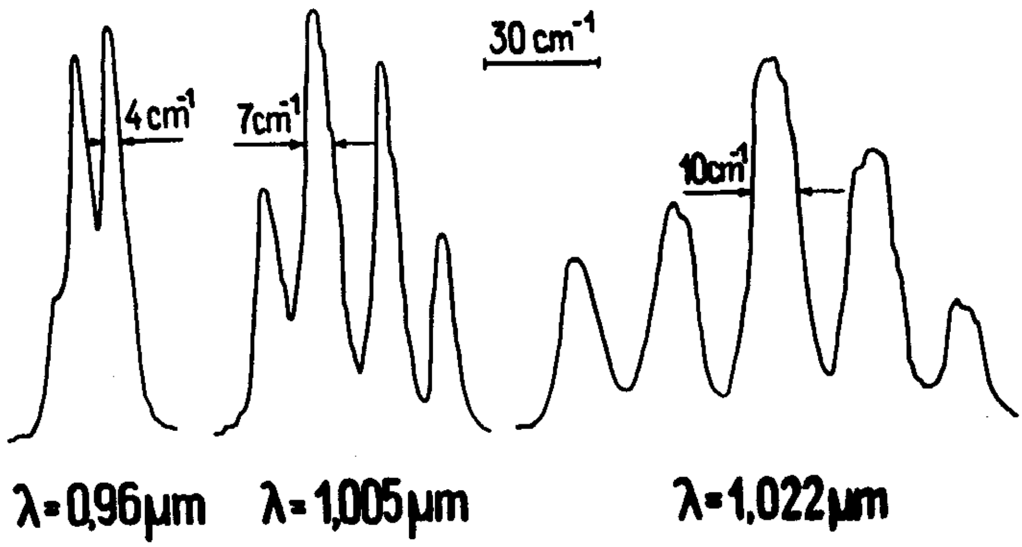

Ps OPO Pumped by TCP

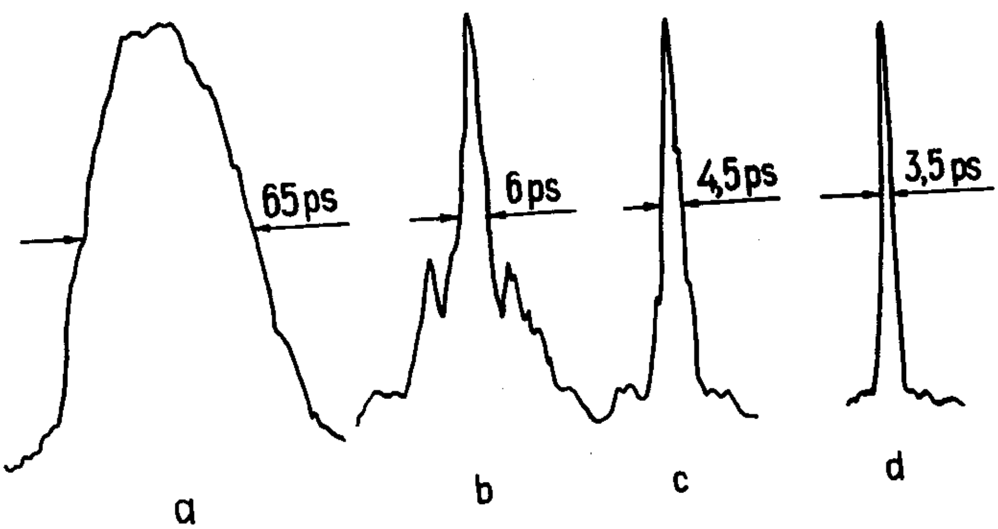

Pulses emitted by the pump laser (a), pulse after compression (b), second harmonic pulse (c) and OPO pulse (d)

β-BaB_2O_4 ps OPO
Experimental Setup

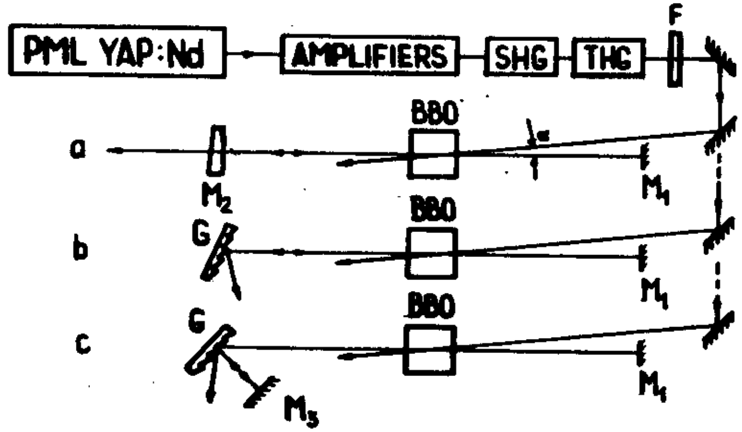

Pump parameters

	λ,nm	E_T,mJ	τ,ps	$\Delta\nu\cdot\tau$
Laser	1079	7	–	–
Amplifiers	1079	50	–	–
SH	540	20	25	4,3
TH	360	8	25	6,5

β-BaB_2O_4 ps OPO. Energy Conversion Versus Pump Intensity

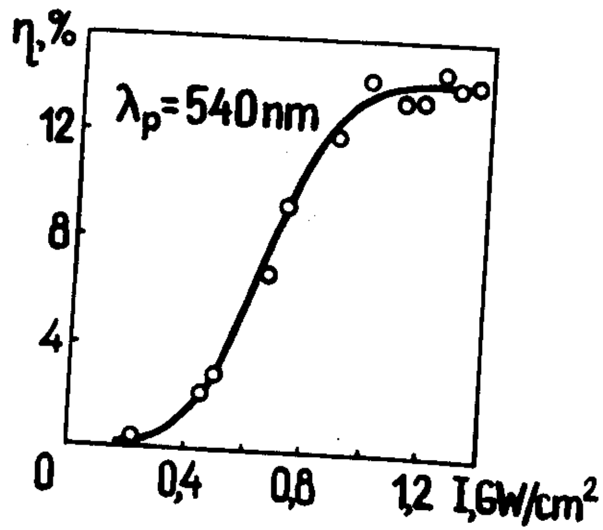

β-BaB_2O_4 ps OPO. Spectrum bandwidth

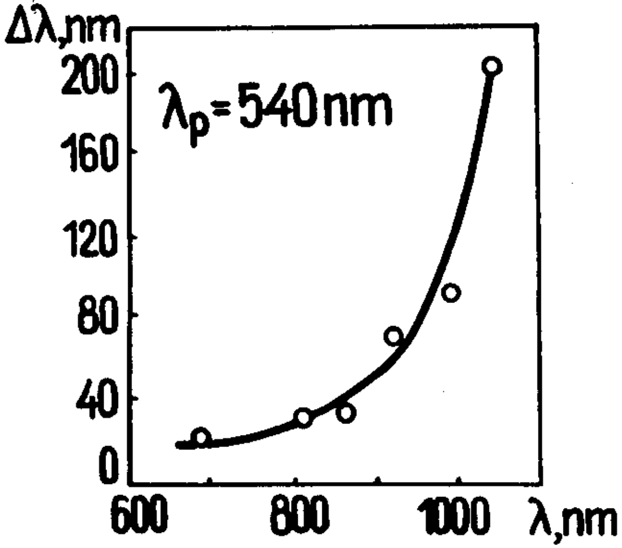

β-BaB_2O_4 ps OPO. Spectrum Bandwidth

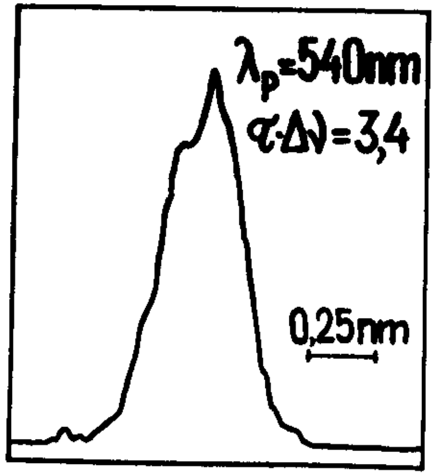

η=1,5%

β-BaB_2O_4 ps OPO. Conversion Efficiency Versus Pump Intensity

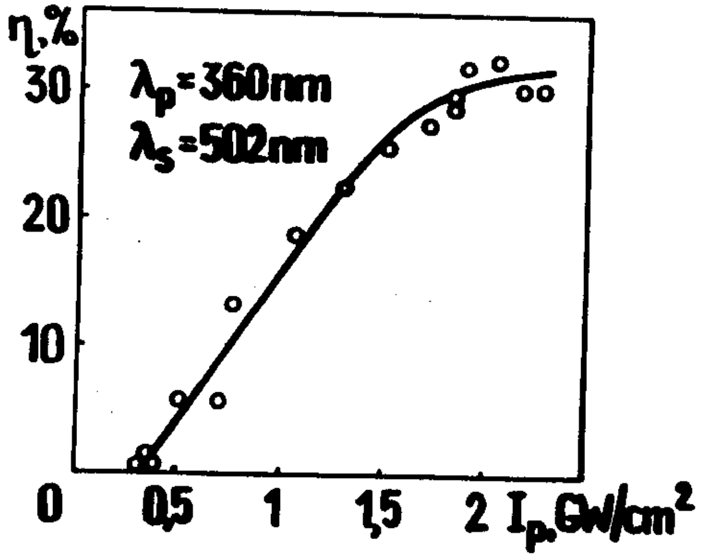

β-BaB_2O_4 ps OPO. Spectrum Bandwidth

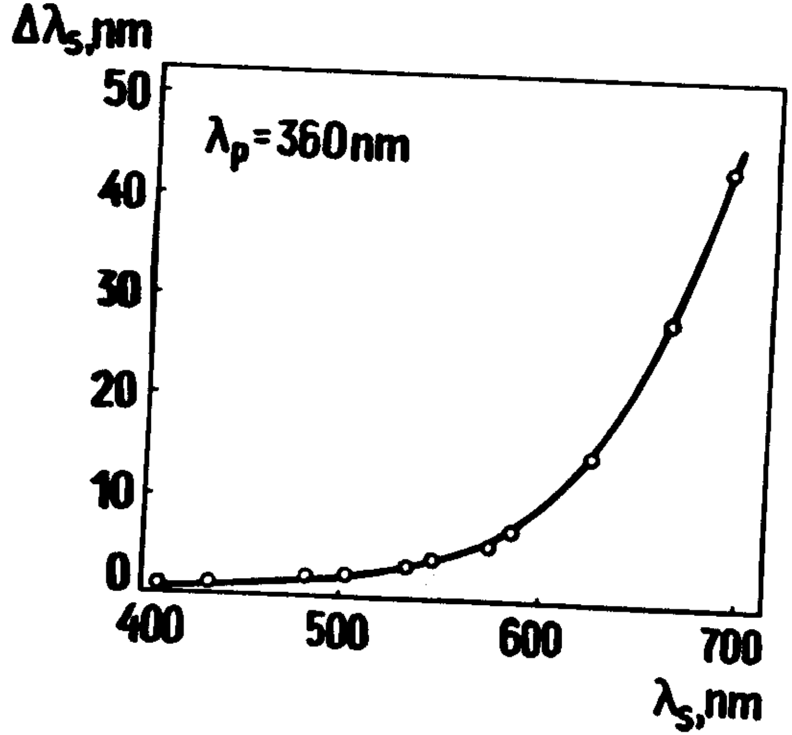

$\beta-BaB_2O_4$ ps OPO. Spectrum Bandwidth

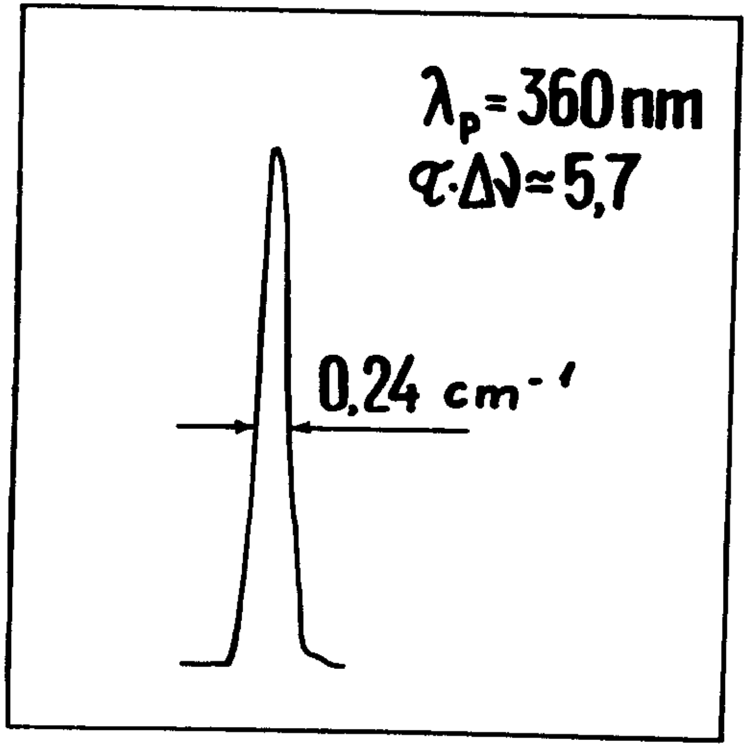

OPO Parameters

Crystal	Length mm	P_{th}, kW	ε_{max}, %	τ, ps	P_s, mW	P_p, kW	$\Delta\nu$, cm^{-1}	Tuning range, μm
$LiNbO_3$	25	21	17,5	15-45	26	29	6-100	0,85-1,4
$Ba_2NaNb_5O_{15}$	10	7	21	7-45	40	44	4-200	0,672-2,56
KTP	6,5	12	17	~40	25	27	10-30	0,95-1,2
$Ba_2NaNb_5O_{15}$ with selective resonator	10	28	8,1	12-45	29	32	≤0,9	0,672-2,56
BBO (λ_p=0,355 μm)	11,8	80	2,2	13-30	5,2	13	10-100	0,59-0,89

Configuration of the cw femtosecond OPO.

(TANG C.L. et. al.)

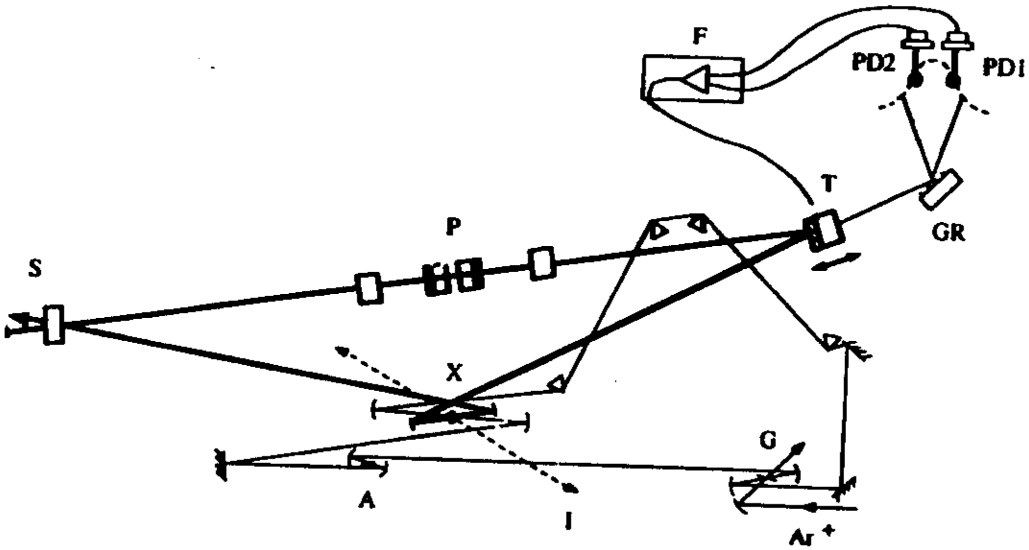

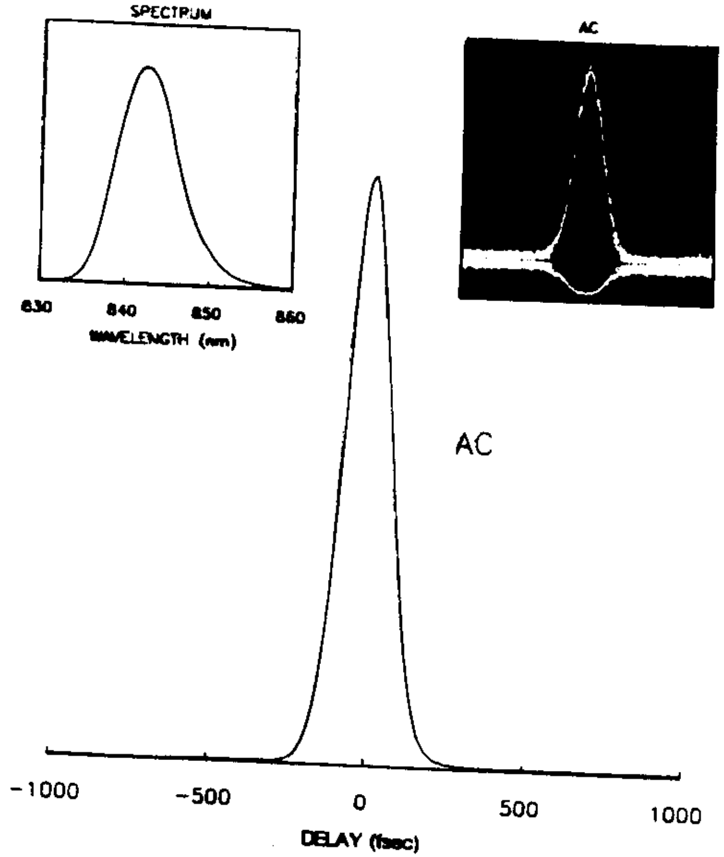

AC of signal pulses at 840 nm for near-zero net cavity GVD; the insets show an interferometric AC envelope (right) and spectrum (left). The pulse width (a sech^2 fit) is 105 fsec. The time–bandwidth product of $\Delta\nu\Delta\tau \approx 0.35$ and the symmetric spectrum are indicative of transform-limited pulses.

(from TANG C.L. et al.)

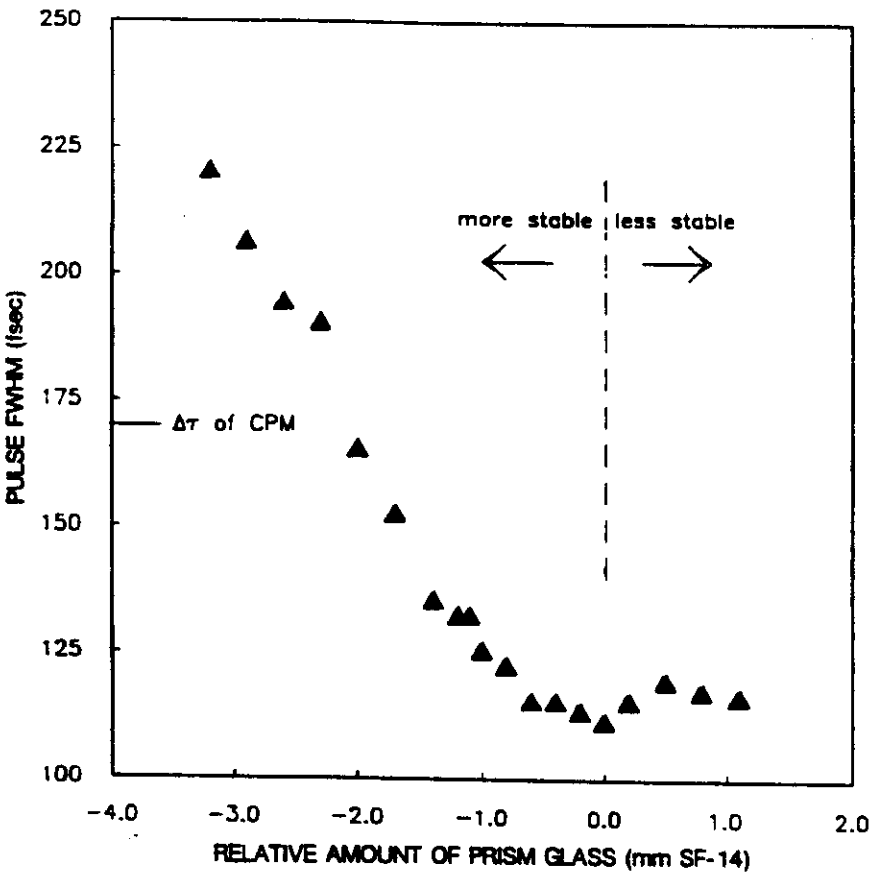

Variation of the signal pulse width with OPO prism lass at 840 nm for a pump pulse width of 170 fsec. In the egion of greater negative GVD, operation is stable with ulse widths of up to 220 fsec.

(from TANG C.L. et. al.)

INTRACAVITY fs $KTiOPO_4$ OPO

(by C.L. TANG et. al. CORNELL U.)

PUMP: CPM dye laser

$\tau_p = 350\,ps$

$P_p = 20\,mW$

$S_p = 1 \div 10\ GW/cm^2$

$p.r.r. = 10^8\,Hz$

OPO: KTP (1.4 mm, o→e+o)

$\alpha \leq 3\%$ (600÷900 nm)

$P_s = 2\,mW \times 2$

$\tau_s = 220\,fs$ (820−920 nm)

$\tau_s = 105\,fs$ (840 nm, disp. comp)

$\Delta\nu \cdot \Delta\tau \simeq 0{,}35 \rightarrow sech^2$

FORECAST:

TUNIBILITY: 720÷4500 nm

$\tau_s|_{min} = 100\,fs$

Key points

- Wave Front Reversal and Chirp Reversal (similarities and differences)
- Requirements for Chirp Reversal Observation (experiments)
- Phase Conjugation and Time-Space-Domain Squeezing

Space and Time-Domain Phase Conjugation

$$a(x,y,t)\cos[\omega_0 t - k_0 z + \varphi(x,y,t)]$$

monochromatic wave	plane wave
$a(x,y)\cos[\omega_0 t - k_0 z + \varphi(x,y)]$	$a(t)\cos[\omega_0 t - k_0 z + \varphi(t)]$
wave front reversal	chirp reversal
$\varphi \to -\varphi$	$\varphi \to -\varphi$, $\dot{\varphi} \to -\dot{\varphi}$

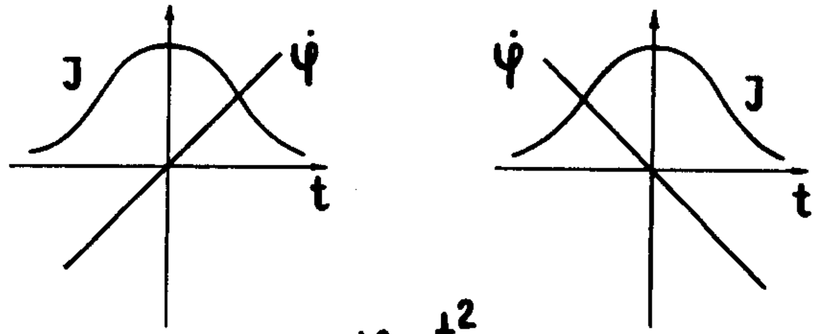

$\varphi \sim t^2$

Phase Conjugation in OPO

$$\omega_1 + \omega_2 = \omega_3$$

$$A_1 = A_{10}\,\mathrm{ch}\,m + \sqrt{\frac{\sigma_1}{\sigma_2}}\,A_{20}^*\,\mathrm{sh}\,m$$

$$A_2 = A_{20}\,\mathrm{ch}\,m + \sqrt{\frac{\sigma_2}{\sigma_1}}\,A_{10}^*\,\mathrm{sh}\,m$$

$$m = \sqrt{\sigma_1\sigma_2}\,A_{30}Z$$

$m \gg 1$, $A_2 = \sqrt{\dfrac{\sigma_2}{\sigma_1}}\,A_1^*$ ⇨ phase conjugation

Chirp Reversal

- J.H.Marburger. Appl. Phys. Lett., 32, 372 (1978).
- A.Yariv et al. Opt. Lett., 4, 52 (1979).

__Chirp reversal of ps and fs pulses__

Requirements for conjugator:

- Nonlinear response

  $\tau_{res}^{NL} \ll \tau_{\text{signal correlation time}}$

- Phase-matching bandwidth

  $\Delta\nu_{P.M.} \gg \Delta\nu_s$

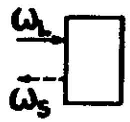

SBS $\quad \tau_R \sim 10^{-10}$ s

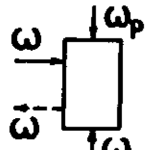

DFWM $\quad \tau_R \sim 10^{-12}$ (ionic) $- 10^{-15}$ s (electronic)

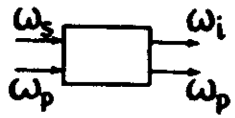

OPA $\quad \tau_R \sim 10^{-15}$ s (electronic)

Spectrum Bandwidth of OPA

$$\omega_3 = \omega_1 + \omega_2 \qquad \ae = \frac{\omega_2}{\omega_3}$$

$$\ae \neq 0{,}5 \qquad \Delta\omega_{OPA} \sim \left(|\nu_{12}|^2 \ell L_{NL}\right)^{-1/2}$$

$$\ae = 0{,}5 \qquad \Delta\omega_{OPA} \sim \left(|k''_{\omega}|^2 \ell L_{NL}\right)^{-1/4}$$

$\lambda = 1\,\mu m$, $1 ps \rightarrow 15\, cm^{-1}$

$10 fs \rightarrow 1500\, cm^{-1}$

OPO Spectrum versus Pump Wavelength

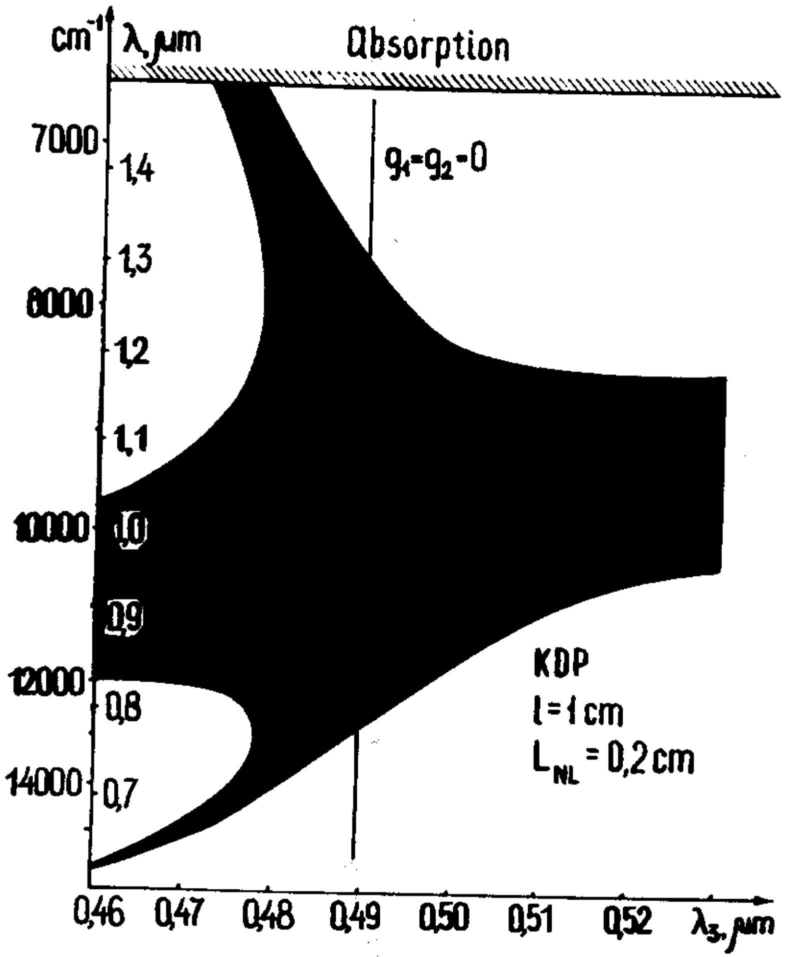

VU | CDA OPA Bandwidth Dependence on Temperature Tuning

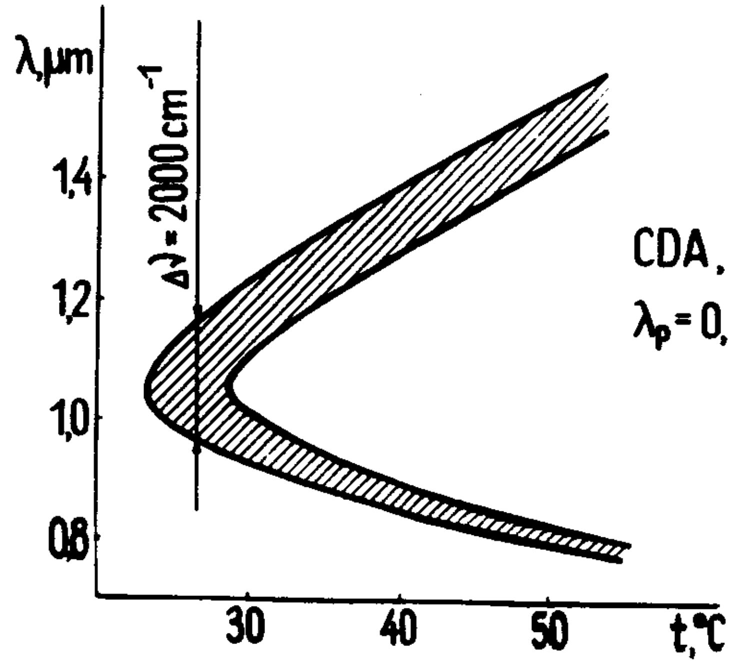

KDP (e-oo) OPO Spectrum

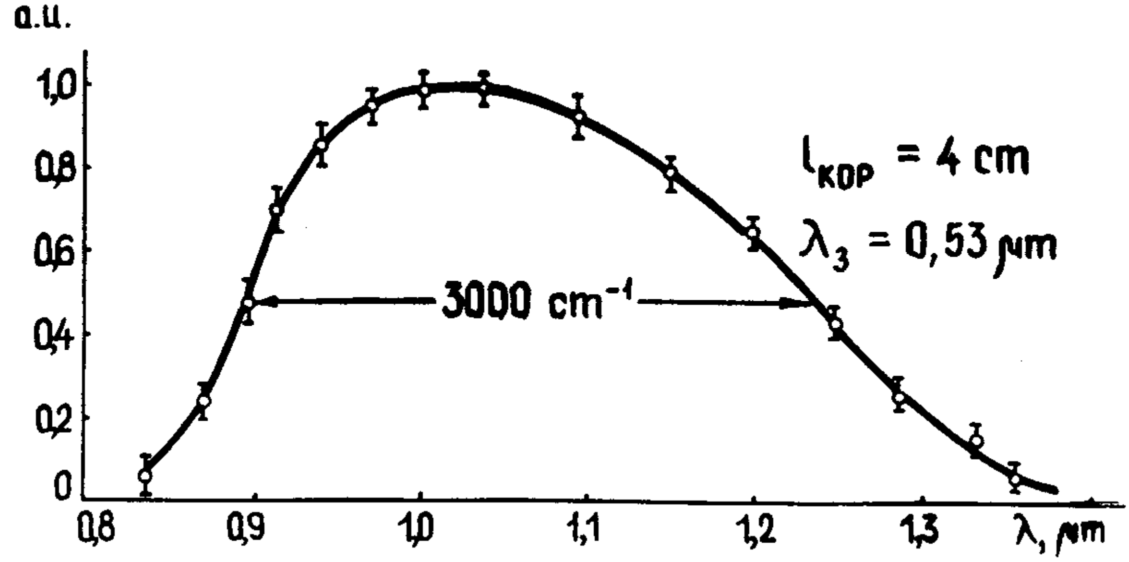

VU Experimental Setup for Chirped ps Signal Parametric Amplification, Chirp Reversal and Compression in Positive GVD Medium

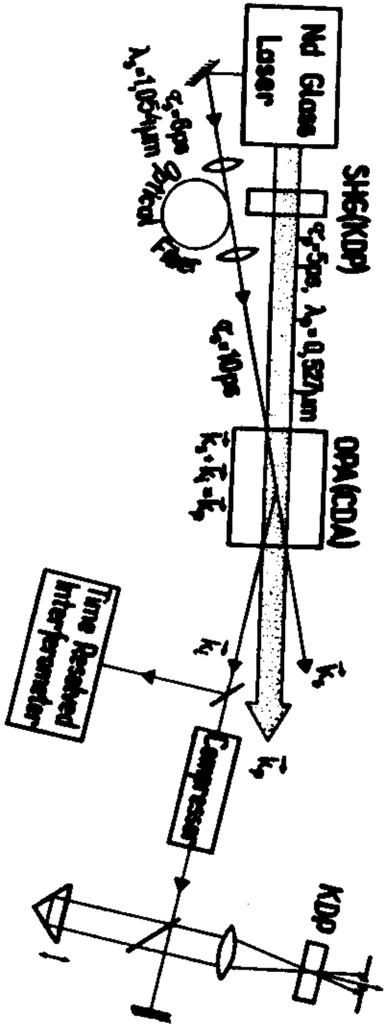

Michelson-Streak-Camera Type Dynamic Interferometer

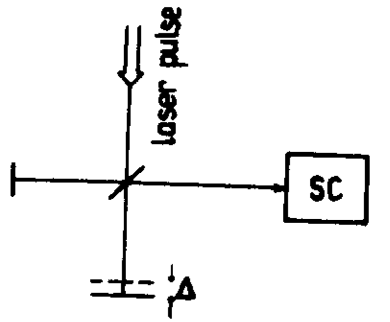

$$\frac{\partial \nu}{\partial t} = \frac{\nu}{m}\frac{dm}{dt}$$

$$\Delta \nu = \frac{1}{2\Delta}$$

CW pumped actively
QS and ML YAG:Nd Laser

VU Compression result

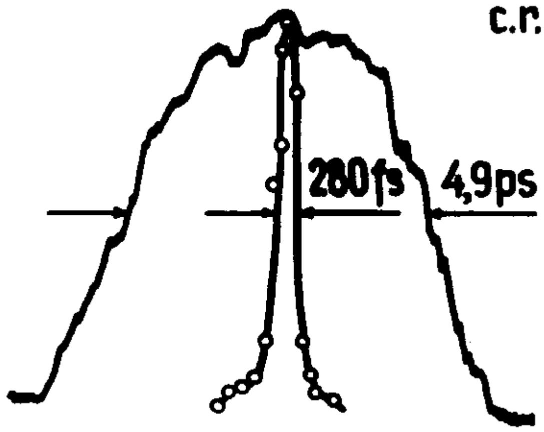

VU Chirp Reversal in CDA OPA

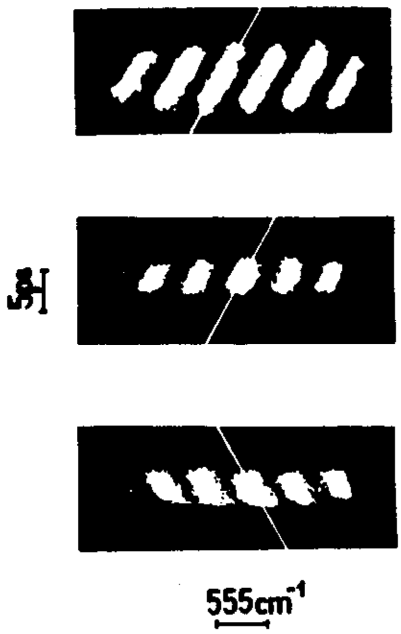

E,mJ	Δν, cm⁻¹	τ, ps	Δν/τ, cm⁻¹/ps	
10^{-4}	400	10	40	single-mode fiber output signal
0,5	200	5	40	amplified signal
0,5	-200	5	-40	phase-conjugated idler

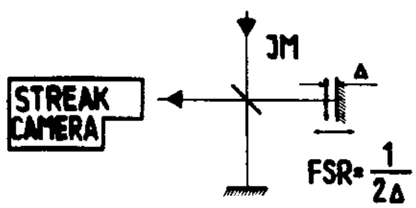

Parametric Chirp Dependence on Degeneracy Value

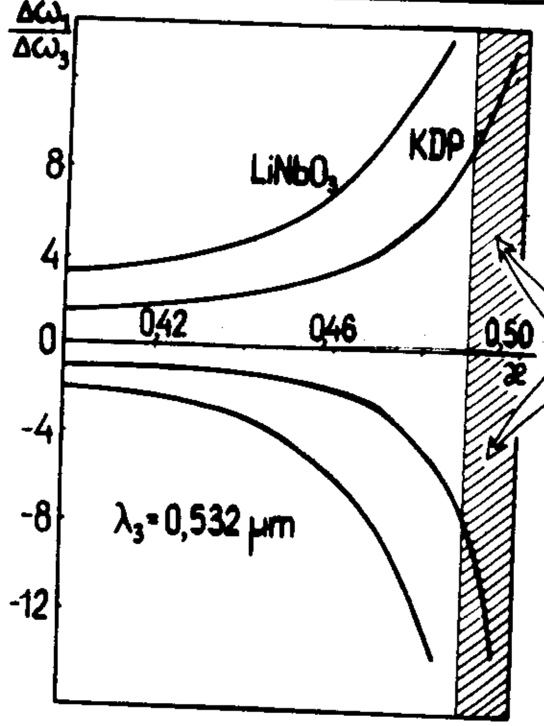

$$\frac{\Delta\omega_1}{\Delta\omega_3}=\frac{F}{1-2æ} \qquad F\ \frac{\frac{dk_3}{d\omega_3}-\frac{dk_1}{d\omega_1}}{\frac{d^2k_1}{d\omega_1^2}\,\omega_3}$$

$$\frac{\Delta\omega_2}{\Delta\omega_3}=1-\frac{\Delta\omega_1}{\Delta\omega_3} \qquad æ=\frac{\omega_2}{\omega_3}$$

Nonlinear chirp region:

$$\frac{\Delta\omega_3}{\omega_3}\geq\frac{1}{10}\,\frac{(1-2æ)^2}{F}$$

	F values			
λ_1, μm	LiNbO$_3$	KDP	CDA	LiIO$_3$
1,06	0,20			-0,21
0,53	0,54	0,16	0,39	0,56
0,35		0,57		
0,26		0,58		

OPO Tuning Curves

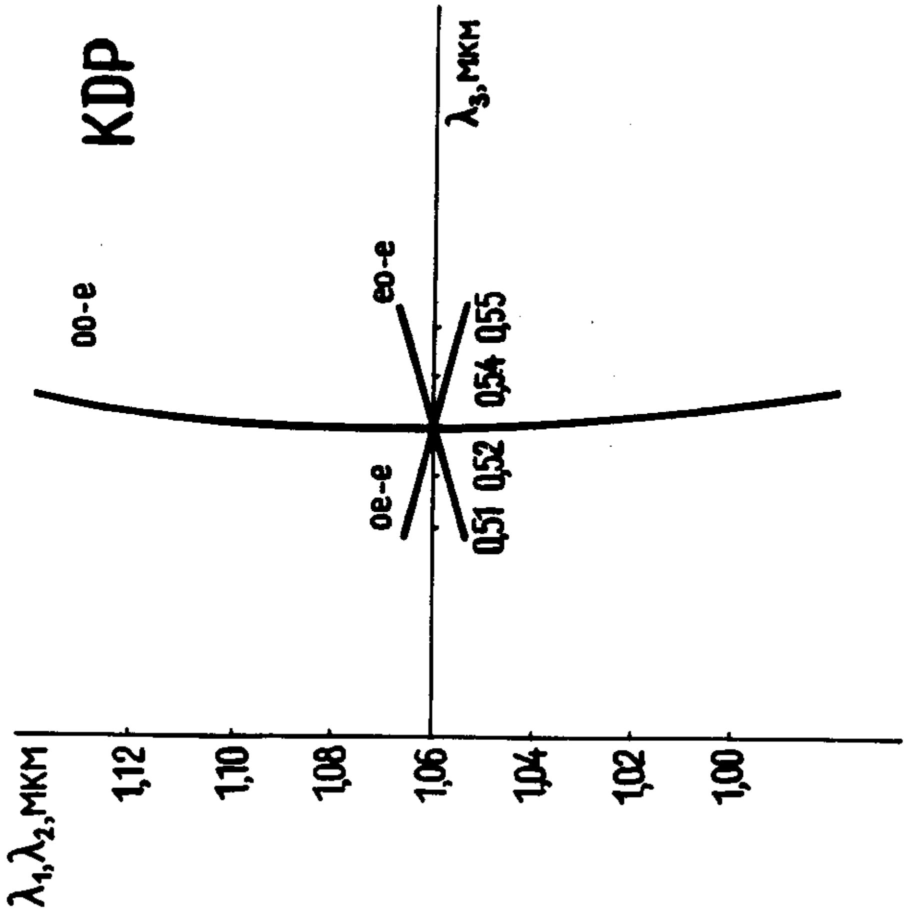

VU Chirp Enhancement Results

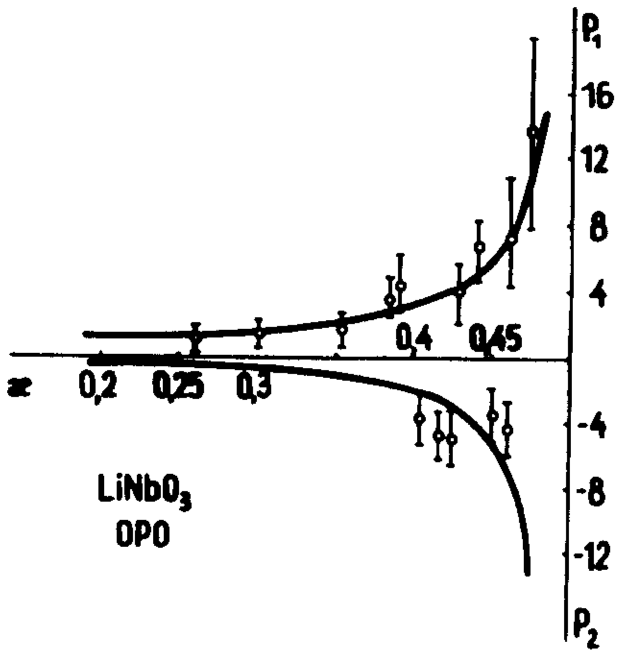

VU Evolution of Pump and OPO Signal Chirp along Train

CW pumped actively mode -locked and Q-switched

YAG:Nd laser
p.r.r. = 10 kHz
τ_p = 60ps

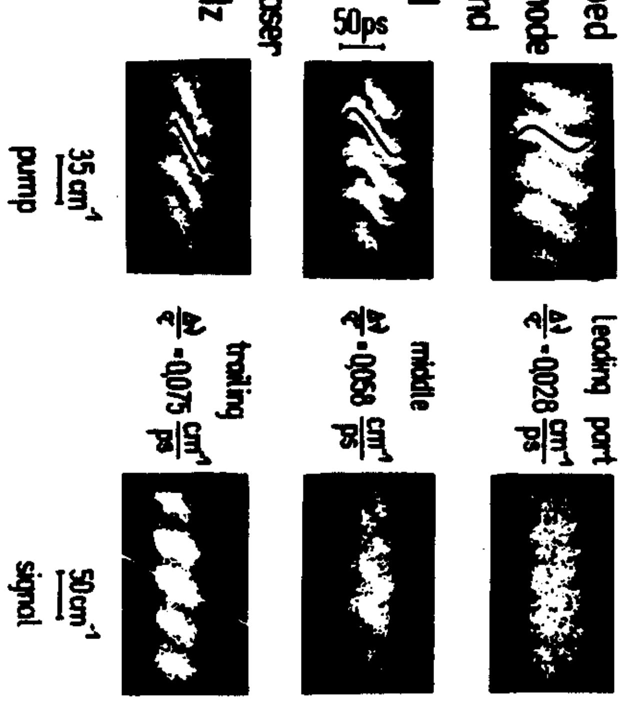

Synchronously pumped OPO $LiNbO_3$

$\frac{\Delta\nu}{\tau} = 0{,}52 \frac{cm^{-1}}{ps}$

VU	Compression Results

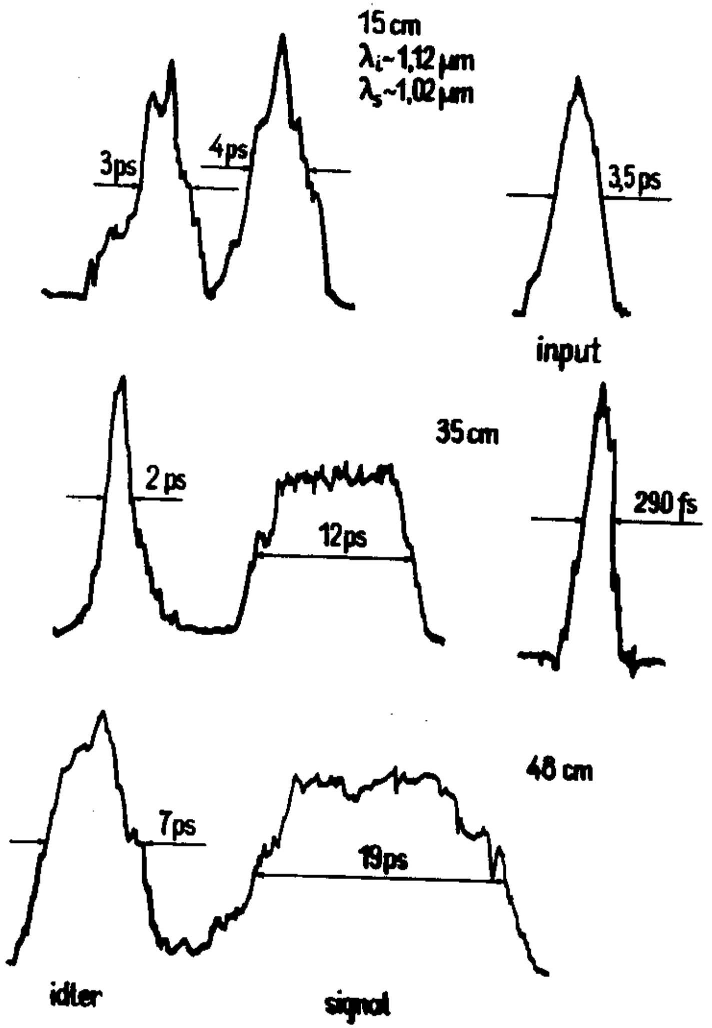

Fs β-BARIUM BORATE OPO with INTRACAVITY CHIRP ENHANCEMENT & PULSE SELFCOMPRESSION

(by A. LAUBEREAU et. al. BAYREUTH U.)

<u>PUMP</u>: SH of FCM Nd:glass

$\tau_p = 0.8\ ps$

TRAIN: 300 pulses

$E_p = 10^{-6}\ J$

$\lambda_p = 527\ nm$

p.r.r. = 15 Hz

<u>OPO</u>: (BBO, $l = 5{,}8\ mm$)

$\Delta\lambda = 700 \div 1800\ nm$

$\tau_p = 65 \pm 7\ fs\ (\lambda = 1076\ nm)$

$\eta = 3\%$

<u>FORECAST</u>:

$\tau_p \Rightarrow 10\ fs$

Phase Conjugation and Squeezing in OPO

Classical analogy

$\omega_1 = \omega_2 = \omega_{3/2}$,   oo-e

$A = A_0 \mathrm{ch}m + A_0^* \mathrm{sh}m$, $m \gg 1$

$A \sim (A_0 e^m + A_0^* e^m) \Rightarrow$ conjugated waves

Suppression of one quadrature component

$A_0 = a_0 + ib_0$, $A = a + ib$

$a = a_0(\mathrm{ch}m + \mathrm{sh}m)$

$b = b_0(\mathrm{ch}m - \mathrm{sh}m)$

$\overline{a^2} = \overline{a_0^2} e^{2m}$, $\boxed{\overline{b^2} = \overline{b_0^2} e^{-2m}}$

Conclusion:

squeezing in OPO is caused by phase conjugation

Verification of Phase Conjugation

Nonlinear mixing

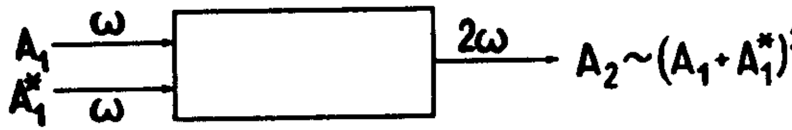

$A_2 \sim \boxed{A_1^2 + A_1^{*2}} + 2\boxed{A_1 A_1^*}$

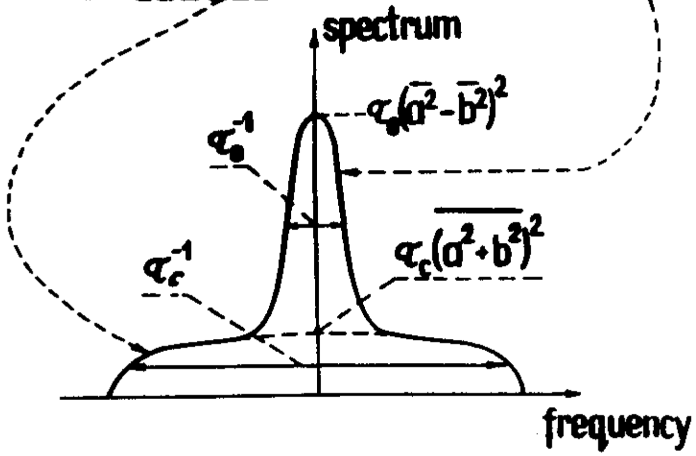

τ_0 - pulse duration

τ_c - correlation time

$\tau_0 \gg \tau_c$ sharp peak in SH spectrum when $\overline{a^2} \neq \overline{b^2}$

VU Phase Conjugation in PPO

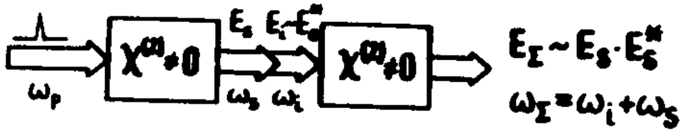

$$E_s \sim e^{i\varphi(t,\vec{r})}$$

$E_\Sigma \sim |E_s|^2$
- free-chirp pulse
- diffraction limited beam

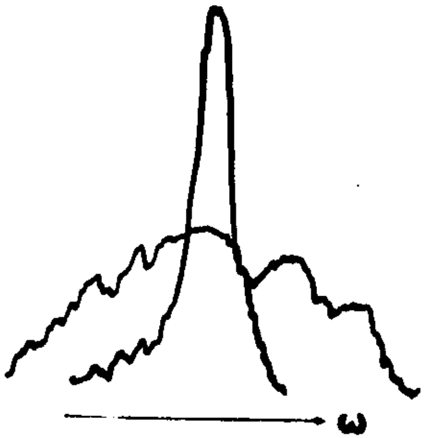

VU Radiation Spectrum with Phase Modulation (b) and with Eliminated One (a)

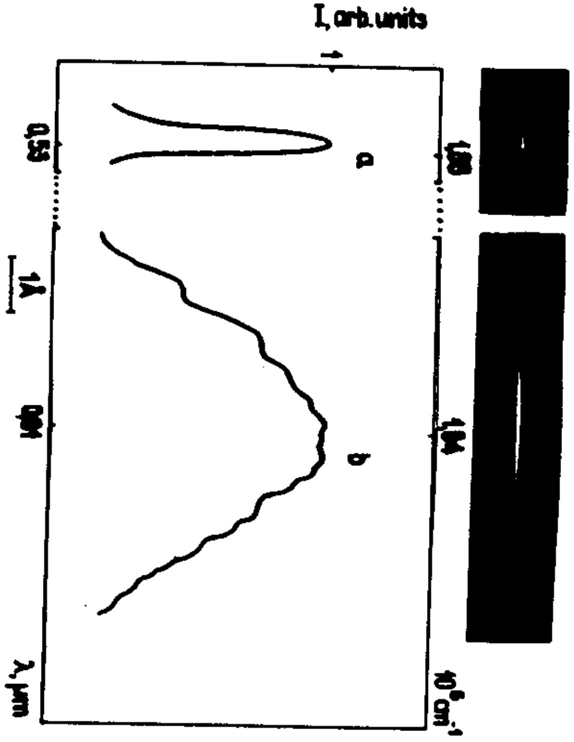

$E_1 = \exp i[\omega_1 t + \varphi(t)]$; $E_2 = \exp i[\omega_2 t - \varphi(t)]$; $E_3 \sim E_1 E_2$

VU	Far-field angular distributions of phase conjugated (1) and nonconjugated (2) waves

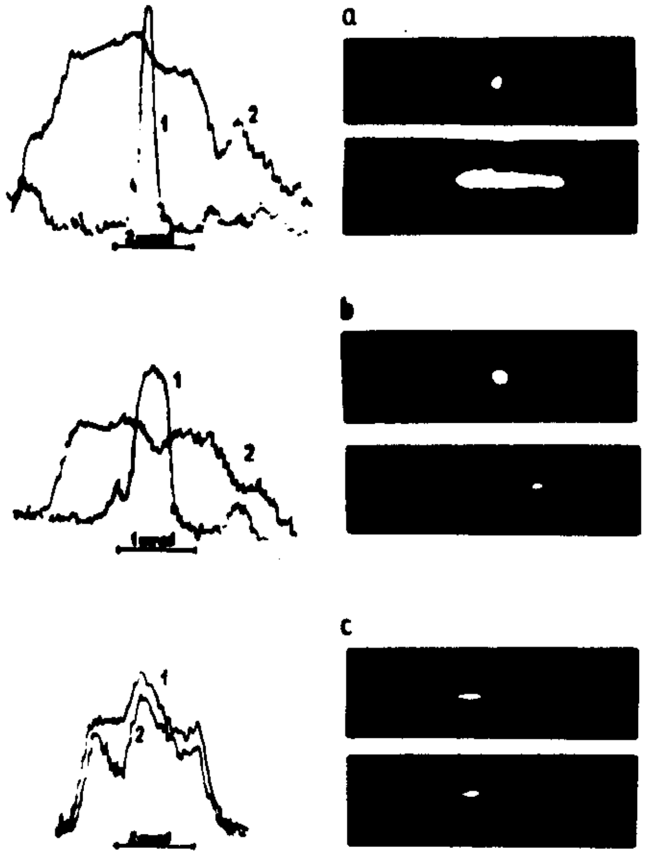

DETERMINATION OF MULTIMODE SQUEEZING

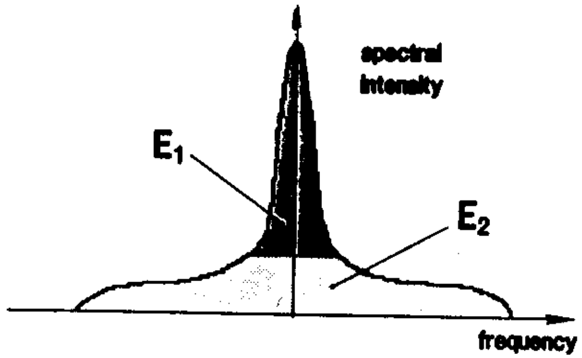

m - parameter of multimode squeezing

$m = E_1/E_2 > \frac{1}{2}$ condition of multimode squeezing*)

$$m = \frac{(1-\varepsilon)^2}{g_F(\varepsilon)(1+\varepsilon)^2 - (1-\varepsilon)^2}$$

$\varepsilon = \overline{b^2}/\overline{a^2}$ conjugation parameter

$\varepsilon = 1$ no conjugation

$\varepsilon = 0$ complete conjugation

$$g_F = \frac{\overline{(a^2 + b^2)^2}}{(\overline{a^2} + \overline{b^2})^2}$$ second order coherence of twin-field

*) S.Kilin. Sov.Opt. & Spectroscopy V.66, p.733 (1989).

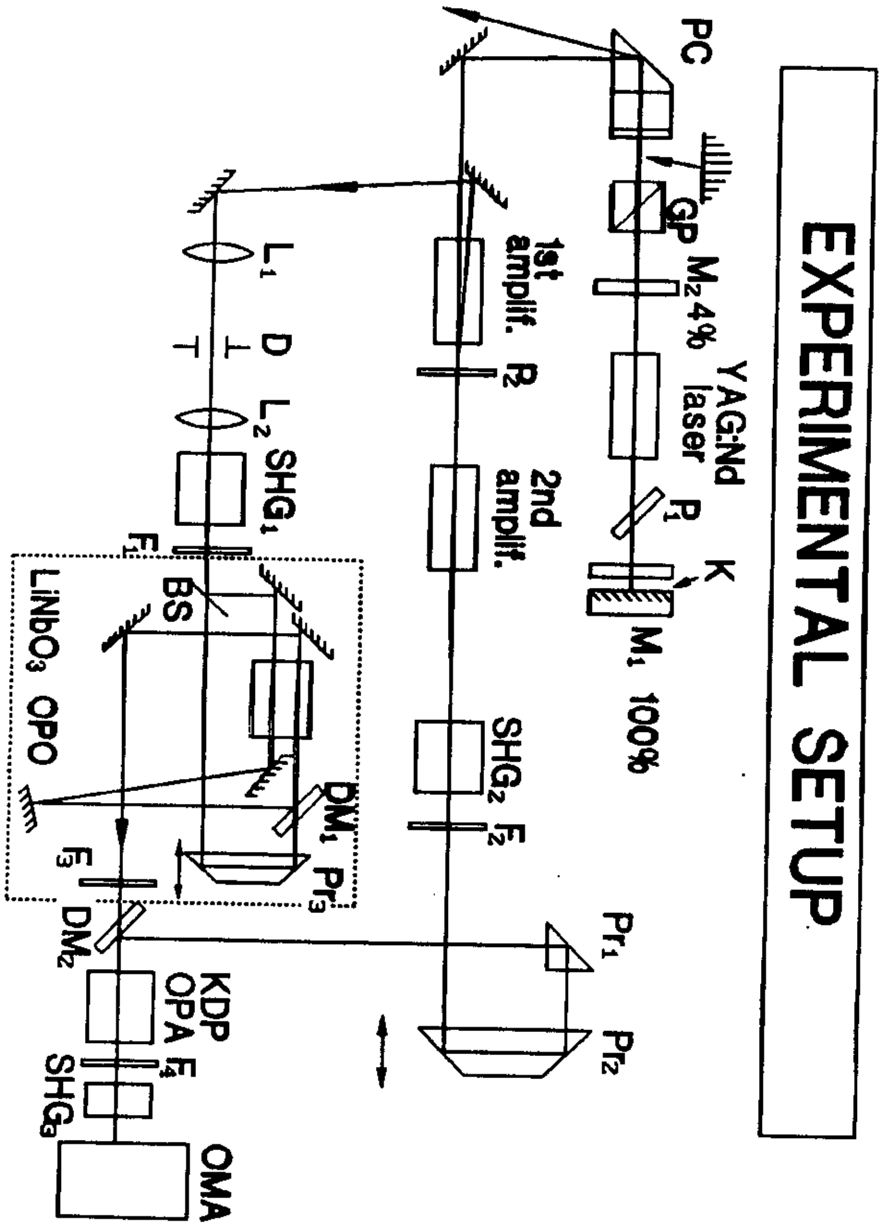

EXPERIMENTAL SETUP
PC
GP
YAG:Nd laser
M_2 4%
P_1
K
M_1 100%
1st amplif.
P_2
2nd amplif.
SHG_2
F_2
Pr_1
Pr_2
L_1
D
L_2
SHG_1
F_1
BS
$LiNbO_3$ OPO
DM_1
Pr_3
F_3
DM_2
KDP OPA
F_4
SHG_3
OMA

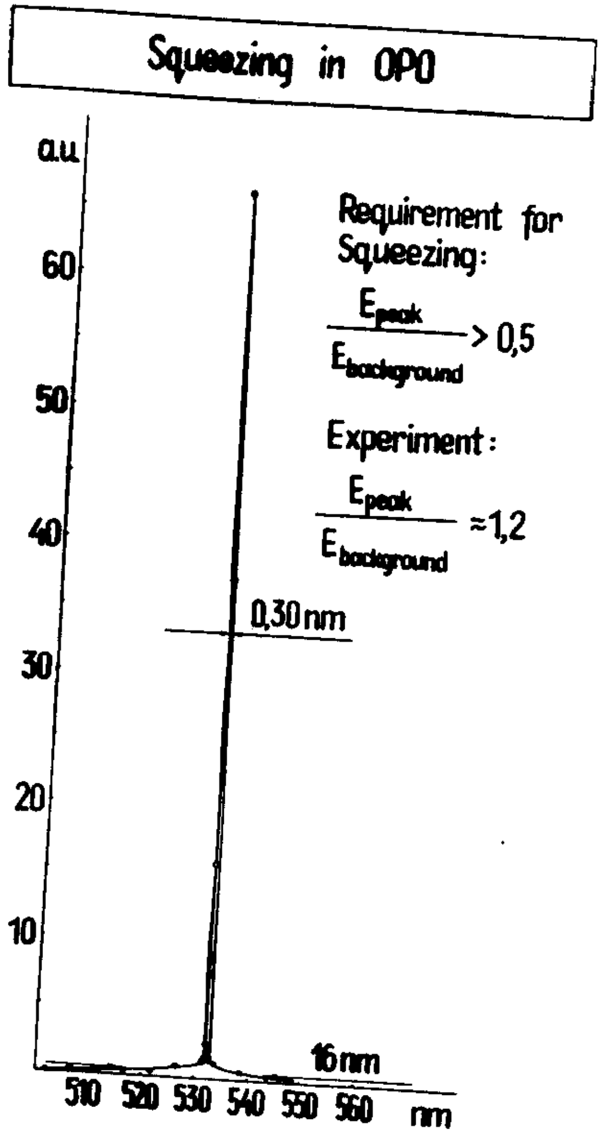

Squeezing in OPO
a.u.
60
50
40
30
20
10
Requirement for Squeezing:
$\frac{E_{peak}}{E_{background}} > 0,5$
Experiment:
$\frac{E_{peak}}{E_{background}} \approx 1,2$
0,30 nm
16 nm
510 520 530 540 550 560 nm

Spatial SH Spectrum of Degenerated KDP OPO

Partial Deconjugation by 20mm of $LiNbO_3$

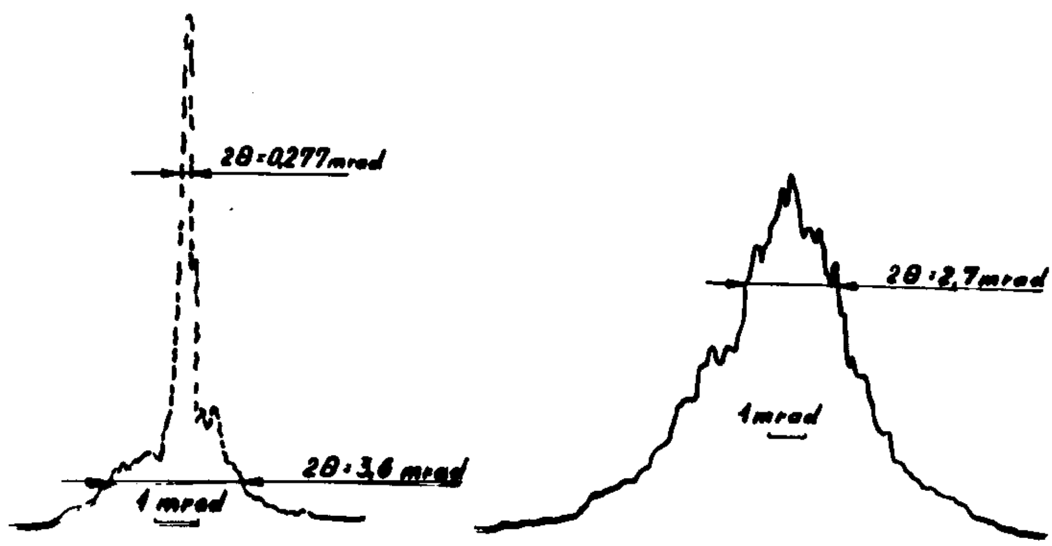

SH SPECTRA OF OPA OUTPUT

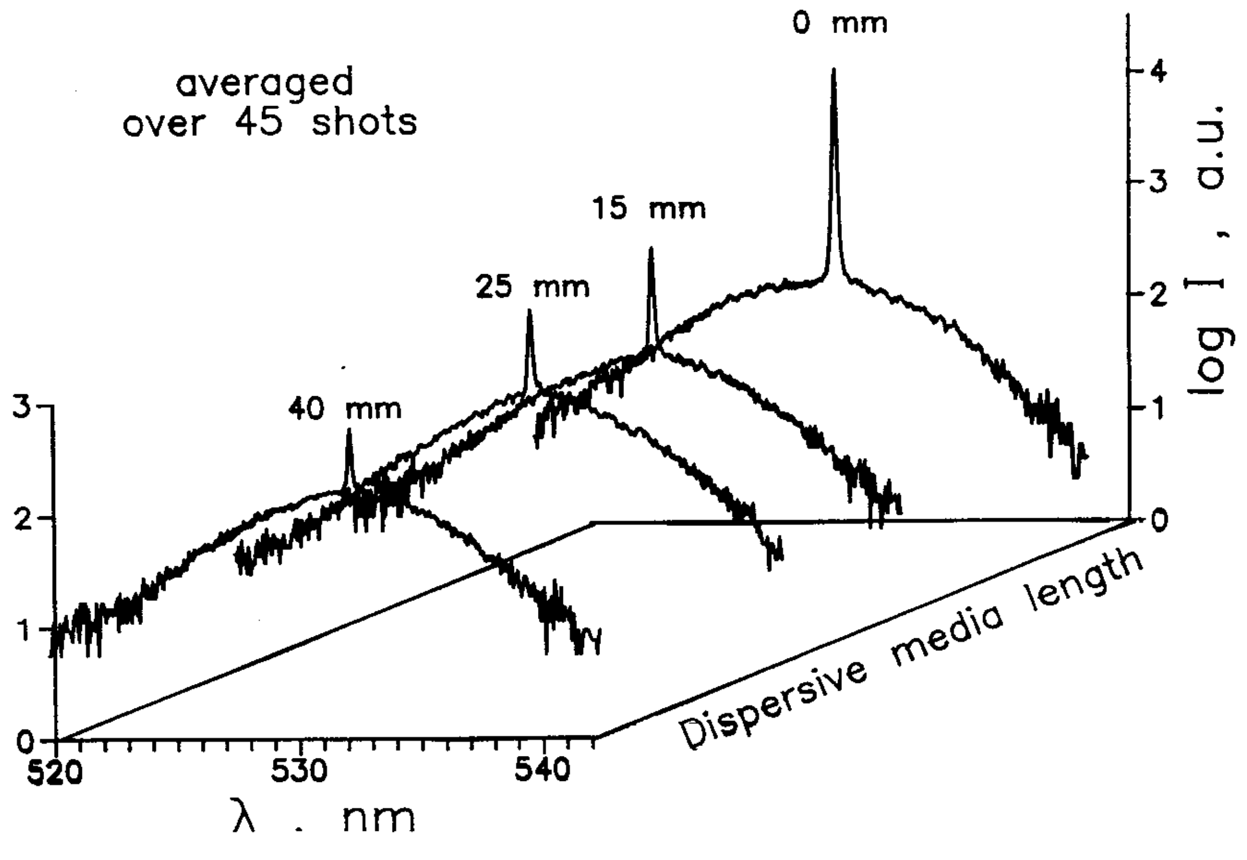

FOUR-PHOTON SODIUM VAPOR PARAMETRIC OSCILLATOR

The Advantages of Nonlinear Gases:

- LARGE LENGTHS
- HIGH OPTICAL DAMAGE THRESHOLD
- SELFRECOVERING
- HIGH TRANSPARENT & HOMEGENEOUS
- PHASE MATCHING
- PRECISE CALCULATIONS

TOPIC:

FIRST EXPERIMENT ON Na-gas OPO

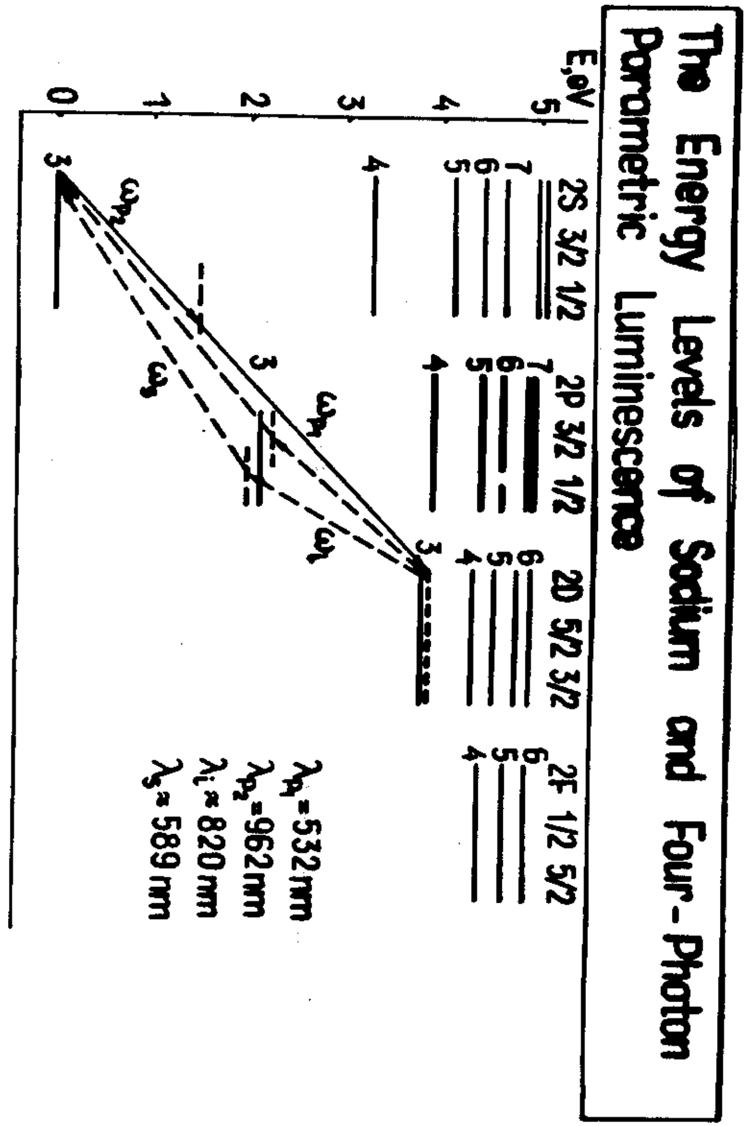

Experimental Arrangement for the Four-Photon Parametric Luminescence Investigations

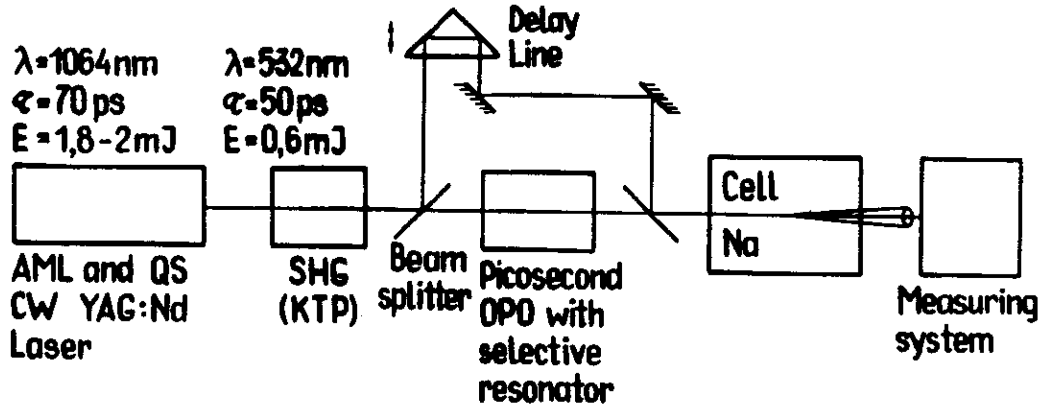

Pump parameters

$\lambda_{p_1}=532nm$ $\Delta\nu_1=0{,}8cm^{-1}$ $E_1=0{,}2mJ$ $P_1=200mW$ $\tau_1=50ps$ $\nu=1kHz$

$\lambda_{p_2}=962nm$ $\Delta\nu_2=0{,}9cm^{-1}$ $E_2=0{,}01mJ$ $P_2=10mW$ $\tau_2=45\text{-}50ps$ $\nu=1kHz$

Three and Four-Photon Parametric Scattering

	Three-photon interaction	Four-photon interaction
Phase matching conditions	$\omega_p=\omega_s+\omega_i$ $\vec{k}_p=\vec{k}_s+\vec{k}_i$	$\omega_{p_1}+\omega_{p_2}=\omega_s+\omega_i$ $\vec{k}_{p_1}+\vec{k}_{p_2}=\omega_s+\omega_i$
Collinear interaction	$\lvert k_s\rvert+\lvert k_i\rvert>\lvert k_p\rvert$ 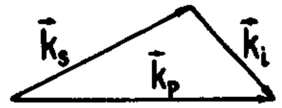	$\lvert k_s\rvert+\lvert k_i\rvert>\lvert k_{p_1}\rvert+\lvert k_{p_2}\rvert$ 
Noncollinear interaction		$\lvert k_1\rvert+\lvert k_2\rvert>\lvert k_{p_1}+k_{p_2}\rvert$ 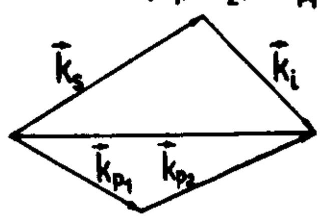

Four-Photon Parametric Luminescence Radiation from Sodium Vapor Cell in Visible Spectral Region during Noncollinear Two-Photon 3S-3D Transition Excitation

$\lambda_{p_1} = 532$ nm
$\lambda_{p_2} = 962$ nm
Concentration $N = 8 \cdot 10^{16} cm^{-3}$

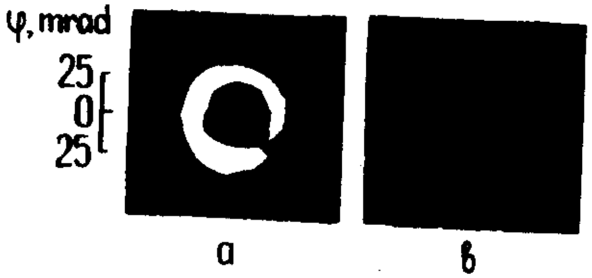

a-angle between pump beams 0 mrad
b-angle between pump beams 17,5 mrad

The Main Formulas for the Calculation of Four-Photon Parametric Luminescence Phase Matching

Phase Matching Conditions

$$\vec{k}_{p1} + \vec{k}_{p2} = \vec{k}_1 + \vec{k}_2 \qquad \omega_{p1} + \omega_{p2} = \omega_1 + \omega_2$$

Cone Angle

$$\cos\varphi = (k_p^2 + k_1^2 - k_2^2)/2k_1k_p$$

$$\vec{k}_p = \vec{k}_{p1} + \vec{k}_{p2}, \qquad |\vec{k}_i| = \frac{n_i(\omega)\omega}{c}$$

Selmeier Equation

$$n(\omega) - 1 = \frac{Nr_e}{2\pi} \sum \frac{f_{nP,J}}{\omega_{nP,J}^2 - \omega^2}$$

N-density of sodium in cm^{-3}
$r_e = 2{,}818 \times 10^{13}$ cm
$\omega_{nP,J}$-energy of the nP_J level in cm^{-1}
$f_{nP,J}$ - the oscillator strength

The Dependence of Four-Photon Parametric Generation Spectral Characteristics on Sodium Concentration

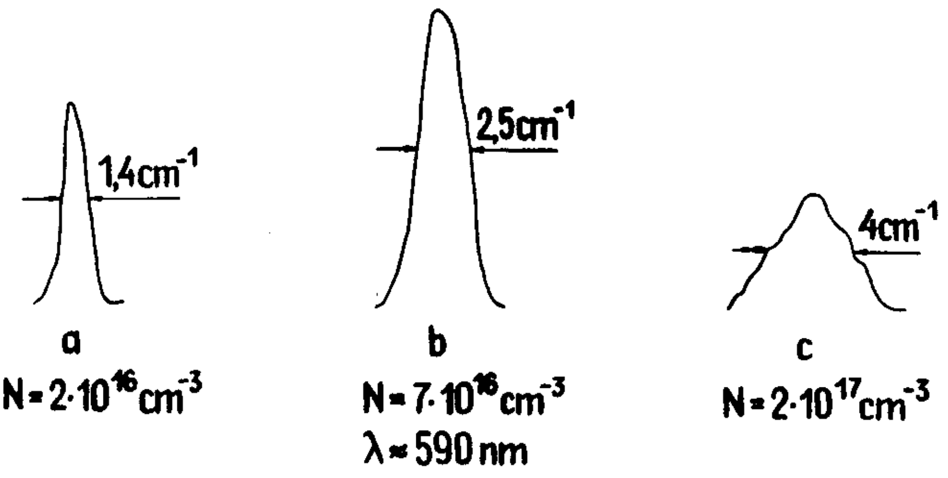

The Types of Cavities Used for Four-Photon Parametric Generator

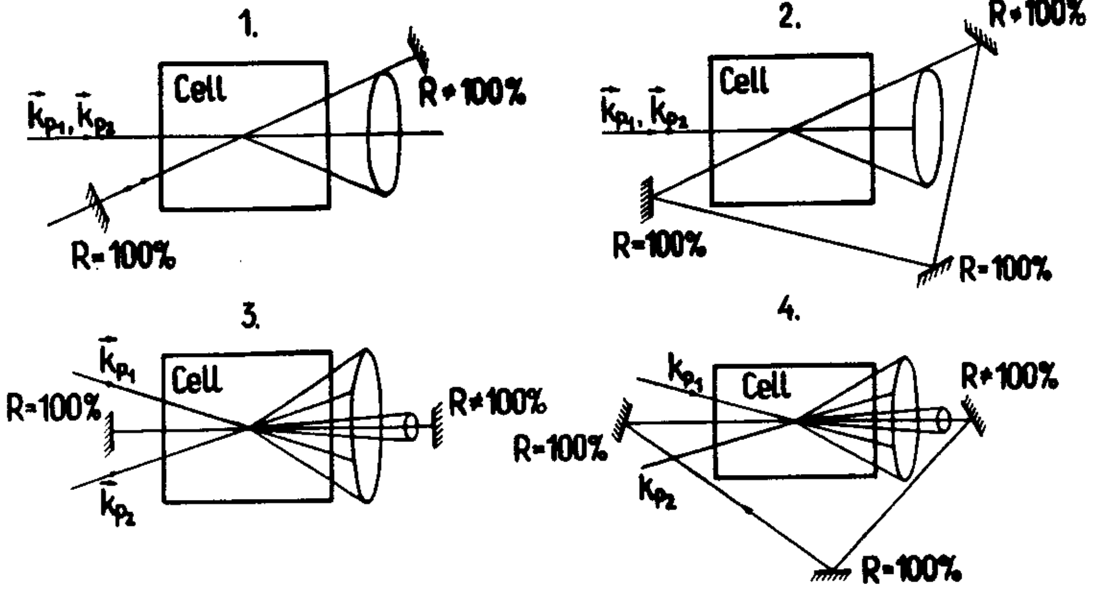

Dependence of the Four-Photon Parametric Oscillator Output Energy on the Cavity Mismatch ΔL

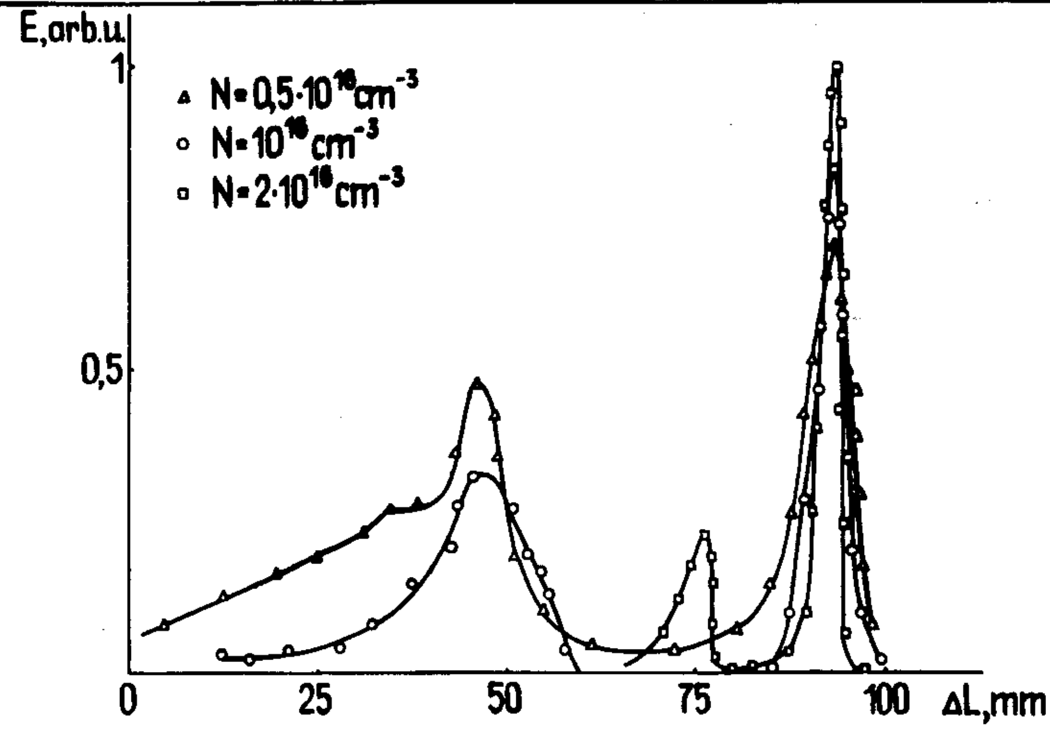

The Pulse Profiles of Four-Photon Parametric Oscillator

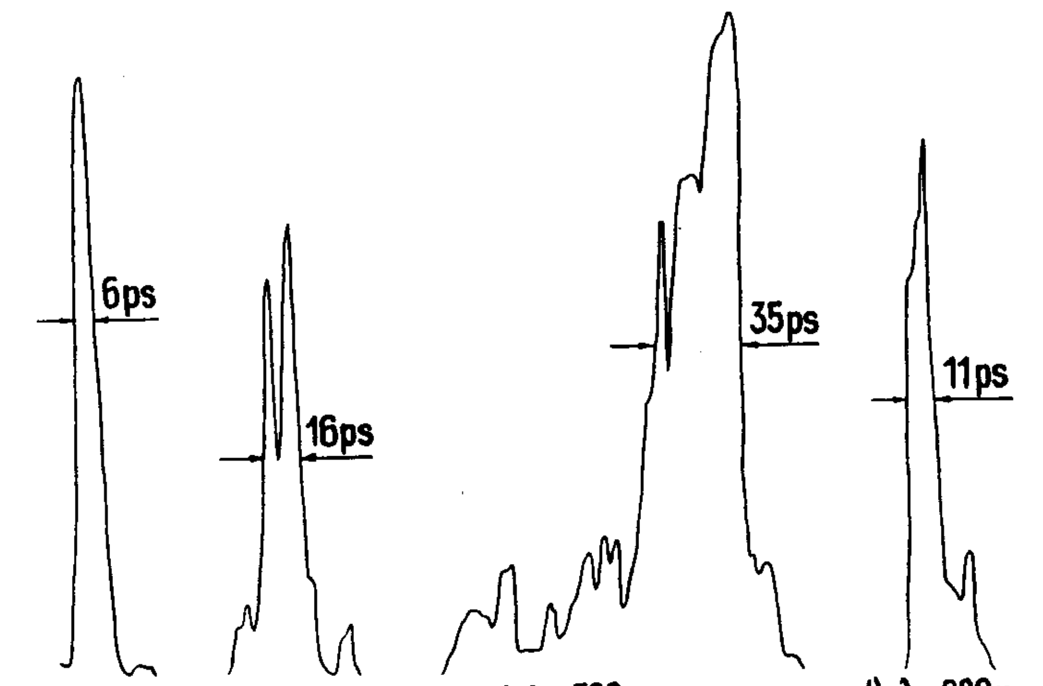

a) $\lambda = 820nm$, $\Delta L_{820} = 0$, $N = 3{,}5\cdot10^{16}cm^{-3}$

b) $\lambda = 820nm$, $\Delta L_{820} = 4mm$, $N = 3{,}5\cdot10^{16}cm^{-3}$

c) $\lambda = 590nm$, $\Delta L_{820} = 0$, $N = 3{,}5\cdot10^{16}cm^{-3}$

d) $\lambda = 820nm$, $\Delta L_{820} = 0$, $N = 10^{16}cm^{-3}$

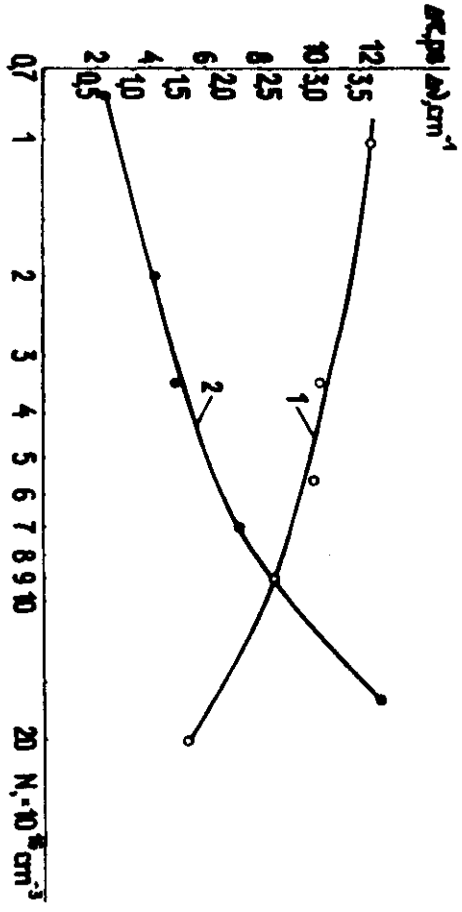

Dependence of the Four-Photon Parametric Oscillator Output Pulse Duration (1) and Spectral Halfwidth (2) on the Concentration of Sodium Vapor

CONCLUSION

- **NEW PHENOMENA OBSERVED**
  - CHIRP REVERSAL
  - CHIRP ENHANCEMENT
  - PULSE SELFCOMPRESSION (SOLITONS)
  - $\chi^{(3)}$ OPO
  - SQUEEZING

- **PARAMETERS ACHIEVED** *)
  - PULSE WIDTH 68 fs
  - LINE WIDTH ~ 10 kHz
  - ENERGY ~ 3 J
  - TUNING ~ 0.3 ÷ 20 μm
  - SQUEEZING ~ 3 dB

*) UNRELATED